Biochimica et Biophysica Acta 1794 (2009) 375–397

Contents lists available at ScienceDirect

Biochimica et Biophysica Acta

journal homepage: www.elsevier.com/locate/bbapap

Review

Protein aggregation kinetics, mechanism, and curve-fitting: A review of the literature

Aimee M. Morris, Murielle A. Watzky *, Richard G. Finke *

Department of Chemistry, Colorado State University, Fort Collins, CO 80523, USA

ARTICLE INFO

Article history:
Received 6 June 2008
Received in revised form 17 October 2008
Accepted 27 October 2008
Available online 11 November 2008

Keywords:
Protein aggregation
Literature review
Kinetics
Mechanism
Curve-fitting

ABSTRACT

Protein aggregation is an important phenomenon that alternatively is part of the normal functioning of nature or, central to this review, has negative consequences via its hypothesized central role in neurodegenerative diseases. A key to controlling protein aggregation is understanding the mechanism(s) of protein aggregation. Kinetic studies, data curve-fitting, and analysis are, in turn, keys to rigorous mechanistic studies. The main goal of this review is to analyze and report on the primary literature contributions to protein aggregation kinetics, mechanism, and curve-fitting. Following a brief introduction, the multiple different physical methods that have been employed to follow protein aggregation are presented and briefly discussed. Next, key information on the starting proteins and especially the products, and any detectable intermediates, involved in protein aggregation are presented. This is followed by tabulation (in the Supporting information) and discussion (in the main text), of the many approaches in the literature striving to determine the kinetics and mechanism of protein aggregation. It is found that these approaches can be broadly divided into three categories: (i) kinetic and thermodynamic, (ii) empirical, and (iii) other approaches. The first two approaches are the main focus of the present contribution, their goal being curve-fitting the available kinetic data and obtaining quantitative rate constants characterizing the nucleation, growth, and any other parts of the overall aggregation process. The large literature of protein aggregation is distilled down to five classes of postulated mechanisms: i) the subsequent monomer addition mechanism, ii) the reversible association mechanism, iii) prion aggregation mechanisms, iv) an "Ockham's razor"/minimalistic model first presented in 1997 and known as the Finke–Watzky 2-step model, and v) quantitative structure activity relationship models. These five classes of mechanisms are reviewed in detail in historical order; where possible corresponding kinetic equations, and fits to aggregation data via the proposed mechanisms, are analyzed and discussed. The five classes of mechanisms are then analyzed and discussed in terms of their similarities and differences to one another. Also included is a brief discussion of selected empirical approaches used to investigate protein aggregation. Three problem areas in the protein aggregation kinetic and mechanistic studies area are identified, and a Summary and Conclusions section is provided en route to moving the field forward towards the still unachieved goal of unequivocal elucidation of the mechanism(s) of protein aggregation.

1. Introduction

The aggregation[1] of proteins such as amyloid-β, polyglutamine, α-synuclein, and prions has been suggested to be intimately associated with neurodegenerative disorders such as Alzheimer's [1], Huntington's [2], Parkinson's [3], and prion [4] diseases, respectively. Aggregation is also a nuisance in industrial applications where it can interfere with the production and characterization of therapeutic polypeptides [5]. Naturally occurring, productive protein aggregation is also important in nature in cases such as the protein fibrillation reaction of $n(\text{G-actin}) \rightarrow (\text{F-actin})_n$, where G-actin is the globular, and F-actin the fibrillar form, of the protein actin.

For the purposes of this review, we will categorize protein aggregation into three classes: (i) *naturally occurring, productive aggregation* as in the $n(\text{G-actin}) \rightarrow (\text{F-actin})_n$ example mentioned. This reaction occurs throughout the human body, as well as in other organisms, and is necessary in controlling the mobility and shape of the cells [6]. Another example of naturally occurring protein aggregation includes the enzyme glutamate dehydrogenase [7–10]. Both actin and glutamate dehydrogenase function with aggregation of a protein in its native state. A second class of aggregation phenomenon can be classified as (ii) *unwanted aggregation in biology*. This class includes

* Corresponding authors.
E-mail addresses: mwatzky@lamar.colostate.edu (M.A. Watzky), rfinke@lamar.colostate.edu (R.G. Finke).

[1] Herein we use the term "protein aggregation" to describe the process of protein monomers reacting to form fibrils and amorphous aggregates. The term "aggregation" has as its chemical dictionary definition: "A process that results in the formation of [groups of atoms or molecules that are held together in any way]." Alternatively, one could use "agglomeration" since it is defined as: "An indiscriminately formed cluster of particles" [McGraw-Hill Dictionary of Scientific and Technical Terms, 6th Ed., McGraw-Hill, New York, 2003]. In short, we use herein the term "protein aggregation" since it is the most common term in the literature and is acceptable under the definition given above.

1570-9639/$ – see front matter © 2008 Elsevier B.V. All rights reserved.
doi:10.1016/j.bbapap.2008.10.016

α-synuclein, amyloid β, polyglutamine, and prions as common examples of proteins that aggregate and are suspected to play a key role in the neurodegenerative diseases Parkinson's [3], Alzheimer's [1], Huntington's [2], and prion [4] diseases, respectively. This type of aggregation is generally believed to involve aggregation of the protein in a non-native state (vide infra). The final class of aggregation phenomenon is (iii) *unwanted aggregation in an industrial setting*. This class of aggregation usually produces amorphous aggregates and its control and understanding is important to the biotechnology industry for keeping proteins in a non-aggregated, bottleable, long-shelf-life form [11].

Because of its importance, the kinetics and mechanism of protein aggregation have been of interest for approximately fifty years [12]. Protein aggregation is, therefore, a topic that has been the subject of numerous other recent reviews, although from perspectives different than herein [13–26]. Of particular interest is the excellent and critical review on the detailed steps of protein aggregation recently published by C. J. Roberts [14], as well as a review on entropy-driven polymerization of proteins by M. A. Lauffer [26]. However, still missing in our opinion among the available reviews of the expansive protein aggregation literature is an analysis and review focusing on models that can fit kinetic data, give useful, quantitative rate constants, and ideally provide mechanistic insight. Key questions to be answered herein include: (i) How many distinct mechanisms actually exist in the literature for protein aggregation? (ii) What is the essence of each mechanism? (iii) Which mechanisms or models have been used to curve-fit kinetic data? (iv) Do any of these mechanisms have similarities to each other? Also, (v) which of the terms used in the sometimes confusing nomenclature[2] in the protein aggregation literature have the same meaning? These are some of the key questions we hope to answer herein. In short, *a main goal of the present contribution is to analyze and report the primary (in our opinion) literature contributions to protein aggregation kinetics, mechanism, and curve-fitting*.

In what follows we have tried to identify key papers in terms of the 5 main classes (*vide infra*) of mechanistic models in the literature, and to trace each (class of) mechanism back to its earliest origins. Our goal is to distill the literature to its essential components, again in our view. We apologize in advance to the authors of literature we were not able to cover in the space available or have somehow inadvertently missed.

We begin with a brief survey of the physical methods used to measure protein aggregation noting whether the methods are direct or indirect, in-situ or ex-situ, and whether the method is able to measure kinetics. Next, we discuss what is known about the starting proteins, products, and intermediates of protein aggregation—since knowing one's products and intermediates is key to rigorous mechanistic science. Third, we tabulate and discuss the main thermodynamic and kinetic based studies we have found that support what turns out to be the 5 main classes of suggested mechanisms of protein aggregation, all in a somewhat historical order. We also briefly discuss empirical approaches that have been used to fit protein aggregation kinetic data. We end with a discussion of what seems to be some of the common pitfalls in attacking the highly complex problem of the mechanism(s) of protein aggregation. We also list some of the important unsolved problems and hence needed future research directions, and then conclude with a Summary and Conclusions section of the highlights of this review.

[2] The nomenclature in the protein agglomeration literature can be confusing since multiple terms are used for more or less the same phenomenon or meaning. Specifically, used more or less equivalently are the terms: induction period and lag phase to indicate the time before measurable aggregation occurs, and the terms elongation, aggregation, fibrillation, and polymerization all meaning what we will term herein as growth. Adding further confusion is the use of the term "heterogeneous nucleation" to mean, we infer, the dictionary definition of "heterogeneous", that is, nucleation of different, new polymeric aggregates on the surface of existing ("heterogeneous") aggregates or polymers. In the extensive, traditional nucleation theory literature, "heterogeneous nucleation" has been used to mean nucleation in two different phases. Another important definition for any nucleation and growth phenomenon such as protein aggregation is the "critical nucleus", and we use this term herein as used in the nucleation theory literature.

Table 1
Physical methods used in the literature to analyze protein aggregation

Method	Direct/ indirect[3]	In-situ/ex-situ	Measure kinetics?	Selected reference(s)
Absorbance	Direct	Concentration dependent[a]	Yes	[149]
Atomic force microscopy	Direct	In-situ	Yes	[149]
Calorimetry	Direct	In-situ	Yes	[27,150]
Circular dichroism	Direct	Concentration dependent[a]	Yes	[151]
Dyes	Indirect	Concentration dependent[a]	Yes	[149,152]
Electron microscopy	Direct	Ex-situ	No	[27,149]
Electron paramagnetic resonance spectroscopy	Indirect	Concentration dependent[a]	Yes	[70]
Flow birefringence	Direct	In-situ	Yes	[153,154]
Fluorescence spectroscopy with an intrinsic fluorophore	Direct	Concentration dependent[a]	Yes	[152]
Fluorescence spectroscopy with an extrinsic fluorophore	Indirect	Concentration dependent[a]	Yes	[152]
Fourier transform infrared spectroscopy	Direct	Concentration dependent[a]	Yes	[27]
Light scattering	Direct	In-situ	Yes	[111,155,156]
Mass spectrometry	Direct	Ex-situ	No	[27,157,158]
Nuclear magnetic resonance spectroscopy	Direct	Concentration dependent[a]	Yes	[127,159]
Quartz crystal oscillator measurements	Direct	Concentration dependent[a]	Yes	[160]
Turbidity	Direct	In-situ	Yes	[149,161]
Viscosity	Direct	In-situ	Yes	[162]
X-ray diffraction	Direct	Concentration dependent[a]	No[b]	[38,149]

[a] By "concentration dependent" we mean this method can be in-situ if the aggregation conditions are within the detection limits of the physical method.
[b] Or "yes" in principle if Synchrotron radiation is used.

2. Advantages and disadvantages of the physical methods used to monitor protein aggregation

The kinetics and products of protein aggregation have been measured using at least 18 different analytical techniques, each having its own intrinsic advantages and disadvantages. Each technique is summarized in Table 1 and discussed in more detail in the Supporting information. The interested reader is also referred to the recent, excellent review by S. E. Bondos that compares the various methods used to detect protein aggregation, with an emphasis on the concentration and volume ranges for each method, and organized by techniques that: (i) detect protein aggregates, (ii) screen buffers to improve protein stability, and (iii) characterize protein aggregates [27]. Indicated in Table 1 is if the physical methods listed there are used as *direct* or *indirect*[3] methods for the systems at hand, and if they can be used *in-situ* or involve *ex-situ* use and sample preparation. In protein aggregation, as with all science, the use of multiple, complimentary, ideally direct, in-situ physical methods is of course preferred.

One notable study comparing six different physical methods (ANS fluorescence, chymotrypsin resistance, congo red binding, light scattering, SDS-PAGE, and sedimentation) has appeared [28]. Each of the different physical methods shows, for the first time (to our knowledge)

[3] We were unable to find a definition for direct vs. indirect physical methods in the literature. Therefore, we will use the term direct physical method to mean a method that measures a property that is directly affected by the aggregation process, while an indirect method measures a property that is only indirectly affected by the aggregation process.

the same kinetic rate constants within experimental error [29], making that study an especially notable one [28].

Table 1 shows that many different methods for measuring protein aggregation exist, each with their own intrinsic advantages and disadvantages. Therefore, the use of as many multiple, complimentary methods as possible when studying the kinetics and mechanism of protein aggregation is critical.

3. Starting proteins, products, and detectable intermediates of protein aggregation

It has long been known that "know your product(s)" is the first rule of rigorous mechanistic science, since the steps in any proposed mechanism must add up to those observed products. We review, therefore, what is generally known vs. not known about the starting proteins, products, and any detectable intermediates of protein aggregation *when fibrils are formed*, as this category involves many important studies of (native and non-native) protein aggregation. While a main goal of this review is to examine protein aggregation mechanisms supported by kinetic data, presentation of a schematic representation of the overall pathway generally proposed for the aggregation (fibrillation) of the proteins is useful for the discussion that follows and is, therefore, shown in Scheme 1.

The starting reactant in protein aggregation is the monomeric form of the protein. However, in the cases of *unwanted aggregation*, there is an issue as to whether the monomer begins in its native form, or in a denatured, more "active" form. Indeed, misfolded proteins are believed to be part of the first steps in the mechanism of unwanted protein aggregation [30]. For example, the natively unfolded protein α-synuclein [31] is found to have an increased ability both to misfold and aggregate under oxidative conditions, such as pathological conditions that result in the overproduction of oxidants [32,33]. Also, A. L. Fink and co-workers have shown evidence for the formation of partially folded intermediates in the aggregation of α-synuclein [34–36]. It is therefore hypothesized that in some cases the protein monomer undergoes a conformational change, leading to higher β-sheet character or to the exposure of "sticky" hydrophobic patches [34], that then gives the monomer a higher propensity to aggregate, causing it to become "active" [14].

The aggregation of the so-called *amyloidogenic proteins* eventually leads to the formation of insoluble fibers, called amyloid fibrils, as the final product. (In some instances, amorphous aggregates, a hypothesized *off-pathway product* [14,37], have also been observed in the aggregation process.) The morphologies of amyloid fibrils obtained from different proteins are remarkably similar [38]. They typically consist of several concentric protofilaments [39], which in turn are formed by (i) one or more β-pleated sheets [38,40] with each β-sheet consisting of (ii) polypeptide β-strands usually arranged in an anti-parallel configuration [41]. M. Sunde et al. reported Synchrotron X-ray diffraction studies on amyloid fibrils obtained from six different proteins [38], and found a "common core structure" among these proteins at least at the level of the protofilament, as represented in Fig. 1. The protofilament is found to consist of a helical array of one or more β-sheets (four β-sheets are shown in Fig. 1) twisted around the protofilament main axis, with their constituent β-strands perpendicular to that axis [38].

An example of perhaps one of the best-characterized protein fibrils comes from the classic sickle cell hemoglobin system. The product that results from the aggregation of sickle cell hemoglobin under solution conditions is a 21 nm diameter fibril consisting of 14 helical strands arranged in 7 twisted double strands (Fig. 2) [42–44]. A 2.05 Å resolution structure of the helically twisted double strand of sickle cell hemoglobin, believed to be a building block, was solved in 1997 [45].

Other proteins such as actin, collagen, and portions of prion proteins have also been well-characterized by X-ray diffraction [46–52]. However, most protein fibrils are hard to obtain in a crystalline form. Nevertheless, fibrils of amyloid β and α-synuclein among others have been extensively characterized by microscopy, solid-state NMR, and modeling studies as detailed in two recent reviews on the structures of amyloid fibrils [53,54]. These extensive characterization studies have lead to a fairly comprehensive understanding of the general structure of protein fibrils that result from protein aggregation, as well as to a more detailed understanding of the structures of specific fibrils originating from proteins such as actin, collagen, prions, amyloid β, and α-synuclein.

While there is no consensus yet as to whether all or some of the intermediate species of protein aggregation are "on" or "off" the amyloid fibril formation pathway [16,37,55,56], there is some

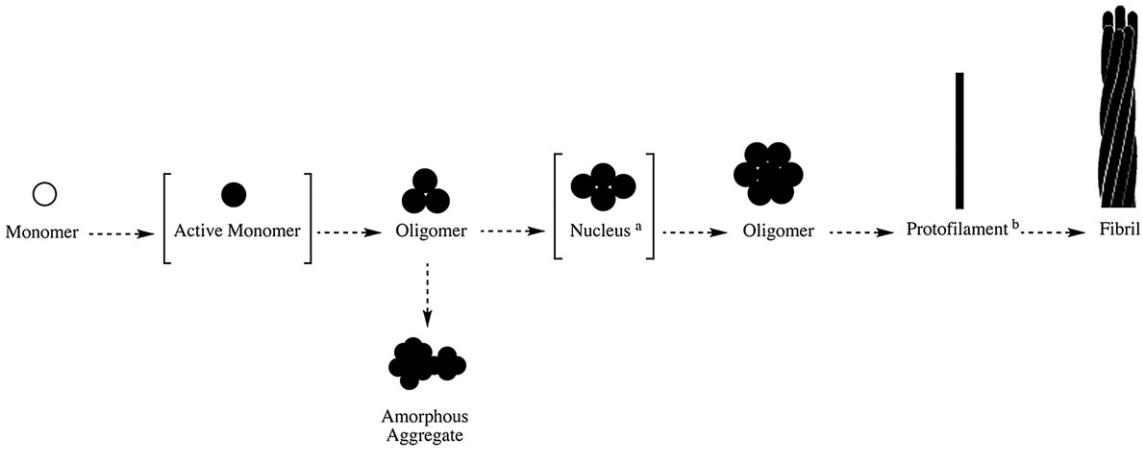

[a]There does seem to be a consensus that protein aggregation occurs via a mechanism that involves nucleation, therefore we included a nucleus formation step.
[b]There does not seem to be a consensus as to whether the protofilament results from an assembly of oligomers or from the addition of monomers, so we chose to represent protofilament formation in a generic way.

Scheme 1. Idealized schematic representation of a general, overall pathway for the formation of protein fibrils, including some possible intermediates [a,b].

Fig. 1. Model of the structure of the common core protofilament in a generic amyloid fibril. This structure was determined using Synchrotron X-ray diffraction on amyloid fibrils of six different proteins. Reprinted from Ref. [38]. Copyright (1997) with permission from Elsevier.

evidence in the literature for the existence of toxic (*vide infra*) intermediate species. Such intermediates can be loosely classified into two categories: (i) soluble oligomers, and (ii) insoluble oligomers or protofibrils. Protofibrils of amyloid-β and α-synuclein have been observed by Lansbury and co-workers using both electron microscopy (EM) and atomic force microscopy (AFM) [57–60]. Fink and co-workers have demonstrated the presence of (soluble) oligomers of α-synuclein using fluorescence studies in conjunction with various other physical methods [34,36,61], and of (insoluble) oligomers of light-chain immunoglobulin using AFM [62,63]. The morphological studies of insoluble oligomers or protofibrils have revealed that these intermediate species contain a ring or annular type structure. Recently, it was suggested that soluble *dimers* of amyloid β are responsible for the toxicity observed in Alzheimer's disease [64].

From their structural characterization, protofibrils of α-synuclein have been proposed to be toxic to neuronal dopamine cells by creating pores within the cell membrane (thus disturbing Ca^{2+} flow and balance [3]), or pores within the membrane of dopaminergic vesicles [65]. Several research groups have also looked at the toxicity of soluble oligomers of amyloid-β and proposed that toxicity could occur by way of (i) reacting with O_2 in the neuronal cell membrane to start a chain of radical reactions leading to the formation of lipid peroxidation products [66]; (ii) generating H_2O_2 within the neuronal cell [67]; (iii) inducing actin/cofilin rods in the neuronal cell [68]; or (iv) by impairing synapse structure and function [64]. In fact in a recent review, Dobson pointed out that smaller ordered aggregates (as compared to disordered or larger ordered aggregates) have a higher proportion on their surface of *hydrophobic* residues normally buried within the interior of the folded protein [69]. These small ordered aggregates are more likely to interact with cellular components such as membranes and receptors and possibly cause disruptive interactions within the cell [69].

However, still needed is more information on the intermediate species and their putative role(s) in toxicity [20]. A possible way to gain information on the intermediate species was recently described in a review covering the technique of high hydrostatic pressure (HHR) for monitoring the aggregation of proteins [24]. HHR is postulated to stabilize and allow for the intermediate species to be isolated [24]. Also, time-resolved methods have been employed to elucidate structural information on the intermediate species of protein aggregation [70–73] and, therefore, insights into the mechanism of protein aggregation (we thank a referee for pointing this out and directing us to the key references).

While there seems to be physical evidence for the starting proteins and final products of protein aggregation, further information is still needed on the (hypothesized) toxic intermediate species [65–68]. With the future development of new techniques and continued interest in this area, more information about intermediate species should become available and allow for further elucidation of the mechanisms of protein aggregation and toxicity [13,20].

4. Thermochemistry of protein aggregation

The aggregation of many biologically important proteins including, but not limited to, tobacco mosaic virus, tubulin, sickle cell hemoglobin, collagen, actin, myosin, flagellin, glutamate dehydrogenase, and α-chymotrypsin have been shown to exhibit a positive enthalpy *and entropy* [26,74]. We refer the readers to the scholarly work contained in references [26] and [74] for the quantitative $\Delta H°$ and $\Delta S°$ values. The positive enthalpy (i.e., endothermic nature) has been verified by calorimetry [26]. The high positive entropy is believed to result from the release of water molecules upon aggregation [26,74,75]. Therefore, protein aggregation is generally an entropy-driven process.

5. Approaches to determine the kinetics and mechanism of protein aggregation

As Scheme 2 illustrates, many approaches exist in the literature for determining the kinetics and mechanism of protein aggregation. Kinetic, thermodynamic, empirical, or other approaches can provide useful information depending upon what one is trying to obtain from

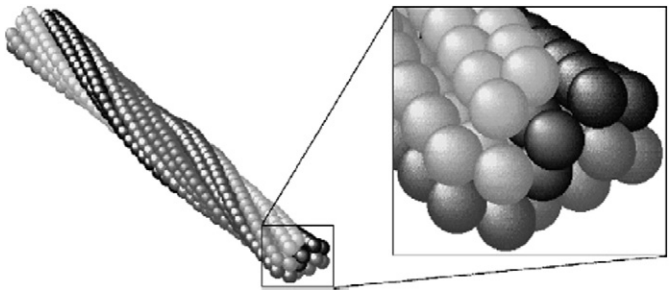

Fig. 2. A schematic representation of the polymerized product of sickle cell hemoglobin. The fibril contains a total of 14 helical strands arranged in twisted pairs. Reprinted from Ref. [148]. Copyright (2006) with permission from Elsevier.

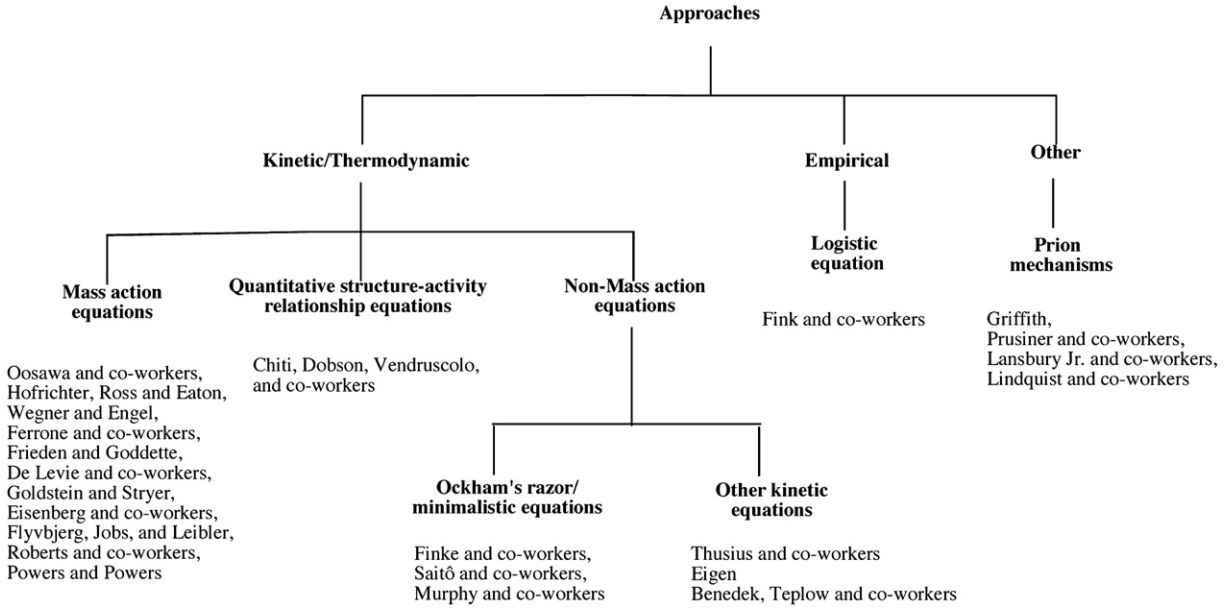

Scheme 2. Literature approaches to determining the kinetics and mechanism for protein aggregation.

the analysis. Herein, we are most interested in being able to curve-fit kinetic data and extract useful information from that data—kinetics being a required part of reliable mechanistic studies. Therefore, the majority of what follows in this review is dedicated to discussing and analyzing the kinetic approaches that have been used in the literature for determining the mechanism of aggregation.

5.1. Historical review of the kinetic and thermodynamic approaches to protein aggregation mechanisms and rate constants

Kinetic and thermodynamic approaches toward determining the mechanism of protein aggregation began approximately 50 years ago with the work of Oosawa et al. [12]. Interest and research has continued to give what we have organized into *five classes of kinetic mechanisms*, as displayed in Table 2 from 50 primary references investigated (Table S1 of the Supporting information). We have distilled down the available literature into what we believe to be the earliest original contributions to each of the different mechanisms proposed. Table 2 that follows is a condensed version of a fuller literature table, Table S1 of the Supporting information, available to the interested reader (a different version of Table 2 was provided in a previous publication [76], but Table 2 displayed herein is more complete). Also provided in Table 2 are the equations, taken directly from the papers under discussion, that one in principle might use to fit experimental data. To avoid confusion, the mathematical symbols and nomenclature original to each paper have been retained in Table 2 (i.e., no attempt was made at this time to express the equations in Table 2 in a common nomenclature, although doing so would simplify the area and is arguably a useful, future goal). Following Table 2 is a discussion of each of the five classes of kinetic mechanisms citing the work of those who have contributed to the understanding and practical applications of the mechanisms discussed. Where possible, we have also provided sample data fits to illustrate the practical applications of the mechanisms and corresponding equations obtained. Finally, we have applied a simplification to the subsequent monomer addition and prion mechanisms that will allow for simplified rate equations to be obtained for future applications.

5.1.1. The subsequent monomer-addition mechanism I. Early contributions

The first key paper probing the mechanism of protein aggregation dates back to 1959 by Oosawa et al. [12]. This paper investigated the aggregation of the native state G-actin protein to F-actin (*vide supra*). The observation was made that the aggregation process resembled a condensation reaction, as aggregation occurs only above a critical concentration [12]. The transformation of G-actin to F-actin as followed by flow birefringence, showed a "First phase characterized by a flat slope… followed by the second phase of a steep slope… expected in cooperative or autocatalytic phenomena" [77], Oosawa notes. The (positive) cooperativity was verified by observing that (i) the initial rate of transformation increased with G-actin concentration, and that (ii) the addition of F-actin produced an immediate transformation of G-actin to F-actin [77]. Connections were drawn to the early polymer literature, and kinetic analyses were performed [78,79]. The resulting rate equation for monomer uptake must be simplified several times with a number of assumptions (including irreversibility), before it can be approximately solved (see entry 1 in Table 2) [78]. In his treatment, Oosawa used a distinction between the concentration of (linear and helical) polymers ($\lambda_l+\lambda_h$) and the concentration of monomer in (linear and helical) polymers (n_l+n_h) [78]. An example of theoretical predictions (or simulations) using Oosawa's analytical expression is shown in Fig. 3. Oosawa's expression, as well as modifications of that expression, has been routinely used over the years by other researchers [86].

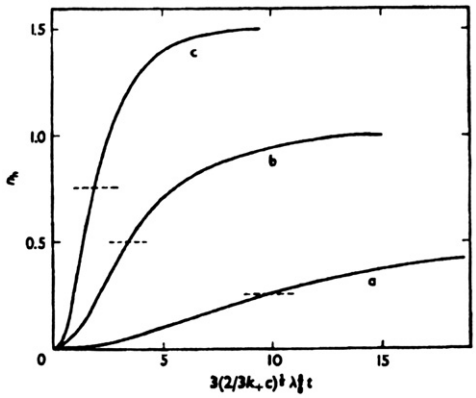

Fig. 3. Oosawa's theoretical curves for actin polymerization, calculated using the equation shown in entry 1 of Table 2. Reprinted from Ref. [78]. Copyright (1962) with permission from Elsevier.

Table 2
Historical summary of the kinetic, thermodynamic, and other models and associated equations for protein aggregation proposed in the literature

Entry	Mechanism	Proposed by	Year	Protein System of Study	Equation given
1	Subsequent monomer addition I. Early contributions	Oosawa et al. [78]	1962	Actin	$\frac{dn_h}{dt} = [k_+\lambda(t) - k_-][f[k'_+\lambda_3(t) - k'_-\lambda_{3h}(t)]dt + 3[k'_+\lambda_3(t) - k'_-\lambda_{3h}(t)] + k_-\lambda_{3h}(t)$ n_h = total concentration of monomers participating in helical polymers k_+ = forward rate constant for the attachment of monomers k_- = reverse rate constant for the detachment of monomers $k'_+\lambda_3$ = forward transformation rate of the ordinary trimers to nuclei of helical polymers $k'_-\lambda_{3h}$ = reverse transformation rate of nuclei of helical polymers to the ordinary trimers Using assumptions and approximations, the above equation simplifies to: $\ln\frac{\left[1+\left(1-\lambda^p/\lambda_0^p\right)^{1/2}\right]}{\left[1-\left(1-\lambda^p/\lambda_0^p\right)^{1/2}\right]} = p(2/pk_+c)^{1/2}\lambda_0^{p/2}t$ p = number of monomers per turn in the helix λ = concentration of monomers λ_0 = initial concentration of monomers c = constant
2		Hofrichter et al. [80]	1974	Sickle cell hemoglobin	$\frac{dM_n}{dt} = \frac{[M]^{n-1}k_f^{n-2}(\sigma K-1)(1-K)}{k_b^{n-3}(\sigma-1)}$ M_n = monomer of critical nucleus size M = monomer k_f = forward rate constant k_b = backward rate constant $K = \frac{k_f[M]}{k_b}$ $K<1$ before nucleation $\sigma K<1$ after nucleation
3		Wegner and Engel [84]	1975	Actin	$\frac{dc_2}{dt} = k_N c_1^2 - k'_N c_2 - kc_1c_2 + k'c_3$ $\frac{dc_i}{dt} = kc_1c_{i-1} - k'c_i - kc_1c_i + k'c_{i+1}$ k_N = rate constant for the formation of the dimer k'_N = rate constant for the destruction of the dimer k = rate constant for the binding of protomers k' = rate constant for the disassociation of protomers c_i = concentration of i-mer with ∞>i>3 Using assumptions and approximations, the above equation simplifies to: $\frac{dc_p}{dt} \approx \frac{k_N(kc_1-k')c_1^2}{k'_N + kc_1 - k'}$ $\frac{dc_p^*}{dt} \approx (kc_1 - k')c_p$ $c_p = \sum c_i$ = concentration of polymers $c_p^* = \sum ic_i$ = *concentration of monomers in incorporated into polymers*
4		Ferrone et al. [83]	1980	Sickle-cell hemoglobin	Homogeneous nucleation: $\frac{dc_p}{dt} = K_N k_+(\gamma c)^n + K_M\phi k_+(c_0-c)(\gamma c)^m$ "Heterogeneous nucleation:" $-\frac{dc}{dt} = nK_N k_+(\gamma c)^n + mK_M/k_+(c_0-c)(\gamma c)^m + (k_+\gamma c - k_-)c_p$ K_N = equilibrium constant for homogeneous nucleation K_M = equilibrium constant for heterogeneous nucleation k_+ = rate of monomer addition k_- = rate of monomer removal γ = activity coefficient of the monomer c_0 = monomer concentration at time 0 c = monomer concentration at time t c_p = number concentration of polymers at time t ϕ = scaling factor for the number of effective nucleation sites n = critical nucleus size
5		De Levie et al. [87]	1983	"Living" polymers	Nucleation + irreversible growth: $J = \frac{dc_n}{dt} + k_f Cc_n \approx k_f Cc_n$ $\frac{-dM}{dt} = (k_f C)^2 c_n t$ Using approximations at short reaction times: $-\Delta M = \frac{1}{2}(k_f C)^2 c_n t^2$ Nucleation + reversible growth: $J = \frac{dc_n}{dt} + (k_f C - k_r)c_n \approx (k_f C - k_r)c_n$ $\frac{-dM}{dt} \approx (k_f C - k_r)^2 c_n t$ Using approximations at short reaction times: $-\Delta M = \frac{1}{2}(k_f C - k_r)^2 c_n t^2$ J = flux $-\Delta M$ = number of monomer consumed in polymer formation

Table 2 *(continued)*

Entry	Mechanism	Proposed by	Year	Protein System of Study	Equation given
5		De Levie et al. [87]	1983	"Living" polymers	$\frac{-dM}{dt}$ = monomer uptake k_f = forward rate constant k_r = reverse rate constant C = monomer concentration c_n = critical nucleus concentration
6		Goldstein and Stryer [90]	1986	Not specified	$\frac{dA_n}{dt} = k_+ A_1 (A_{n-1} - A_n) + k_- (A_{n+1} - A_n)$ when $n<s$ $\frac{dA_n}{dt} = g_+ A_1 (A_{n-1} - A_n) + g_- (A_{n+1} - A_n)$ when $n>s$ A_n = polymer of length n A_1 = monomer s = seed k_+ = forward rate constant prior to the formation of seed k_- = reverse rate constant prior to the formation of seed g_+ = forward rate constant after the formation of seed g_- = reverse rate constant after the formation of seed
7	Reversible association	Eisenberg [7,96]	1970	Glutamate de-hydrogenase	$c = \Sigma c_i = \frac{c_1}{(1-Kc_1)^2}$ with $K = K_i = \frac{c_{i+1}}{c_i c_1}$ $M_w^0 = M_1 \sqrt{1+4Kc}$ c = total concentration of the enzyme c_i = concentration of the species P_i c_1 = concentration of monomer M_w^0 = weight-average molecular weight M_1 = molecular weight of monomer
8		Thusius [8]	1975	Glutamate de-hydrogenase	$\Delta A = \Delta A^0 e^{-\frac{t}{\tau}}$ $\frac{1}{\tau} = k_a \left[\left(\frac{1+4C_T}{K'} \right)^{\frac{1}{2}} - 1 \right] K + k_d$ A = total free association sites τ = relaxation time k_a = association rate constant k_d = dissociation rate constant C_T = total concentration $K = \frac{k_a}{k_d}$ K' = K times the molecular weight of the monomer
9	Prion aggregation mechanisms	Eigen[a] [97] Prusiner [4]	1996 1991	Prion Protein	$\frac{d[A]}{dt} = F_A - k_{-A}[A] - k_{AB}[A] - \frac{k_T[A]}{K_M + [A]}[B]$ $\frac{d[B]}{dt} = -(k_{BA} + k_{-B})[B] + k_{AB}[A] + \frac{k_T[A]}{K_M + [A]}[B]$ A = normal form of the host protein B = pathogenic form of A F_A = constant metabolic formation of A k_{-A} = metabolic decomposition of A k_{-B} = metabolic decomposition of B k_{AB} = noncatalytic conversion of A to B k_{BA} = noncatalytic conversion of B to A k_T = turnover number K_M = Michealis–Menton constant
10		Eigen[a] [97] Lansbury et al. [103]	1996 1993	Prion Protein	Rate of nucleus formation: $\frac{d[B_n]}{dt} \approx k'_F (\sigma q)^{n-2} [B]^2$ Growth following nucleus formation: $\sum_{p \geq n} p[B_p] \approx k_F k'_F (\sigma q)^{n-2} [B]^3 \frac{t^2}{2}$ $\sigma q = \frac{k'_F [B]}{k'_D} b1$ (prior to critical nucleus) $q = \frac{k_F [B]}{k_D} N1$ (after critical nucleus) B = non-pathogenic monomeric protein with pre-prion conformation n = minimal nucleus size required for indefinite progression of aggregate formation i = size prior to critical nucleus formation p = size after critical nucleus formation k'_F = forward flux rate parameter prior to critical nucleus formation k_F = reverse flux rate parameter after the critical nucleus formation k'_D = reverse flux rate parameter after critical nucleus formation k_D = reverse flux rate parameter after the critical nucleus formation

(continued on next page)

Table 2 *(continued)*

Entry	Mechanism	Proposed by	Year	Protein System of Study	Equation given
11	Subsequent monomer addition mechanism II. Later contributions	Flyvbjerg et al. [108]	1996	Tubulin	$\frac{dc_1}{dt} = f_0 c^{n_0} - f_1 c^{n_1} c_1 + b_2 c_2 - d_1 c_1$ $\frac{dc_i}{dt} = f_{i-1} c^{n_{i-1}} c_{i-1} - f_i c^{n_i} c_i + b_i c_i + b_{i+1} c_{i+1} - d_i c_i$ $\frac{dv}{dt} = f_k c^{n_k} c_k$ $\frac{dM}{dt} = f_{k+1} cv$ c = monomer concentration c_i = number concentration of the ith relatively stable intermediate n_i = number of monomers added to form the (i+1)th intermediate k = number intermediate assembly stages of the nucleus v = number concentration of nuclei M = amount of mass polymerized f_i = forward rate constant b_i = backward rate constant d_i = disintegration rate constant
12		Benedek, Teplow et al. [109]	1996	Amyloid-β	$nL_f = \sqrt{\frac{mk_e c^*}{k_n}}$ $N_f = c_0 \sqrt{\frac{k_n}{mk_e c^*}}$ n: number of monomers (per unit length) in the fibril L_f: final length of the fibril m: number of monomers in the micelle c: concentration of protein c^*: critical micelle concentration k_n: nucleation rate constant k_e: elongation rate constant N_f: number of fibrils c_0: initial protein concentration
13		Ferrone [113]	1999	Not specified	$\frac{dc_p}{dt} = J^* c^*$ $\frac{d\Delta}{dt} = Jc_p$ $c^* = K_{n^*}$ $c^{n^*} J^* \approx J \approx k_+ c$ Using approximation at short reaction times: $c_p = J^* c^* t$ $\Delta = \frac{1}{2} J J^* c^* t^2$ Which can be written as: $c_0 - c(t) = \frac{1}{2}(k_+ c)^2 c^* t^2$ c_p = concentration of polymers J = net elongation of the nucleus J^* = rate of elongation of the nucleus Δ = concentration of polymerized monomers $\Delta(t) = c0 - c(t)$ k_+ = elongation rate constant K_{n^*} = equilibrium constant for nucleation n^* = critical nucleus size
14		Roberts et al. [120]	2007	Not specified	$C_M = [N] + [I] + [U] + \sum_{i \geq 2} [R_i] + \sum_{i=1}^{\delta} i \sum_{j=x}^{n^*-1} [A_j R_i]$ C_M: total monomer concentration "[ ]": concentration symbol N: native state monomer I: intermediate state monomer R_i: reversible oligomer of i monomers δ: number of monomers in each growth event n^*: size at which condensation steps begin x: nucleus size A_j: aggregate composed of j monomers $A_j R$: reversibly associated A_j and R
15	"Ockham's razor"/ minimalistic 2-step model[b]	Finke et al. [29,76,89]	1997 2008	Amyloid β, α-synuclein, poly-glutamine, prions	$[A]_t = \frac{\frac{k_1}{k_2} + [A]_0}{1 + \frac{k_1}{k_2 [A]_0} e^{(k_1 + k_2 [A]_0) t}}$ or $[B]_t = [A]_0 - \frac{\frac{k_1}{k_2} + [A]_0}{1 + \frac{k_1}{k_2 [A]_0} e^{(k_1 + k_2 [A]_0) t}}$ A = monomeric protein B = aggregated, autocatalytic form of the protein k_1 = rate constant for nucleation k_2 = rate constant for growth
16		Saitô et al. [127]	2000	Human calcitonin	$f = \frac{\rho\{\exp[(1+\rho)kt] - 1\}}{\{1 + \rho \exp[(1+\rho)kt]\}}$ f = fraction of calcitonin in the fibrillar form ρ = dimensionless value to describe the ratio of k_1 to k $k = k_2[A]0$

Table 2 *(continued)*

Entry	Mechanism	Proposed by	Year	Protein System of Study	Equation given
17		Murphy et al. [134]	2006	Insulin	$A = \frac{k_s \cdot N_i\left(e^{t\left(k_s + k_f \cdot N_i\right)} - 1\right)}{k_s \cdot e^{t\left(k_s + k_f \cdot N_i\right)} + k_f \cdot N_i}$ A = concentration of amyloidogenic species N_i = initial concentration of non-amyloidogenic species t = time k_5 and k_f = rate constants
18	Quantitative structure–activity relationship models	Chiti, Dobson et al. [135]	2003	Amyloid proteins	$\ln(v_{mut}/v_{wt}) = A\Delta Hydr. + B\left(\Delta\Delta G_{coil-\alpha} - \Delta\Delta G_{\beta-coil}\right) + C\Delta Charge$ v_{mut} = aggregation rate of mutant v_{mt} = aggregation rate of WT A,B,C = experimentally determined coefficients ΔHydr. = change in hydrophobicity resulting from the mutation $(\Delta\Delta G_{coil-\alpha} - \Delta\Delta G_{\beta-coil})$ = propensity to convert from α-helical to β-sheet structure ΔCharge = overall change in charge as a result of the mutation
19		Chiti, Dobson et al. [136]	2004	Amyloid proteins	$\log(k) = \alpha_0 + \left\{\alpha_1 I^{\text{hydrophobicity}} + \alpha_2 I^{\text{patterns}} + \alpha_3 I^{\text{charge}}\right\} + \left\{\alpha_4 E^{\text{pH}} + \alpha_5 E^{\text{ionic strength}} + \alpha_6 E^{\text{concentration}}\right\}$ k = aggregation rate I = intrinsic factors E = extrinsic factors hydrophobicity = normalized sum of hydrophobic contributions from each residue patterns = alternating behavior of hydrophobic and hydrophilic residues charge = absolute value of the net charge of the protein pH = pH of the solution ionic strength = ionic strength of the solution concentration = protein concentration

[a] These equations are not provided in the original reference but were later derived by Eigen.
[b] This model is subsequently referred to as the Finke–Watzky (F–W) model.

In 1974, Hofrichter, Ross, and Eaton applied the subsequent monomer addition mechanism to the kinetics of sickle-cell hemoglobin gelation [80]. The authors distinguished nucleation from polymerization as shown in Scheme 3 where M is the monomer, M_n is a polymer of length n, k_f and k_b are the forward and backward rate constants respectively, and n^* denotes the critical nucleus size (*vide infra*). The constant that describes the addition steps during nucleation is assumed to be less than one ($K = k_f[M]/k_b < 1$), but more than one during polymerization ($K' = \sigma K > 1$). That is, the addition steps are assumed to be thermodynamically unfavorable until a critical nucleus is formed (nucleation), but then thermodynamically favorable after nucleus formation i.e., during (polymerization) [80]. The authors introduced an expression for the rate of formation of the critical nucleus (see entry 2 in Table 2) [80], where the critical nucleus represents the least thermodynamically stable species in solution [81,82], that is, the minimum sized oligomer capable of initiating further growth [82]. Also, the authors noted, "The time course of the reaction suggests that this mechanism must involve either a nucleation or an autocatalytic process" [80].

In 1980, during further studies of sickle-cell hemoglobin gelation induced by photolysis, Ferrone et al. ruled out the Hofrichter et al. mechanism due to its inability to predict the shape of the early portion of the aggregation curve. In order to account for the observed "extreme autocatalysis" and strong concentration dependence of the 10th time (the time required to complete one-tenth of the reaction), the authors proposed a new mechanism in which, in addition to homogeneous nucleation, "heterogeneous nucleation" also takes place on the surface of existing polymers [83]. The authors propose individual rate equations for homogeneous and heterogeneous nucleation solvable by numerical integration (see entry 4 of Table 2) [83]. The concept of "heterogeneous nucleation" was a novel and important contribution to the protein aggregation area [83]. An alternative view of "heterogeneous nucleation" might be *seeded autocatalytic growth*. (Experimentally, no one has shown whether the nuclei are forming on the surface of an existing aggregate or if growth is simply occurring on the surface of that same aggregate. The distinction is whether a monomer vs. a critical nucleus is being added to the growing fibril.)

In 1975, Wegner and Engel applied the subsequent monomer addition model to the formation of F-actin, with the exception that the equilibrium constant for the formation of a dimer ($\sigma K = k_N/k_{N'}$) is different from that for each subsequent monomer addition step ($K = k/k'$) [84]. This is shown in Scheme 4, where M is the monomer, M_n is a polymer of length n, k_N and $k_{N'}$ are the forward and reverse rate constants for the formation of a dimer, and k and k' are the forward and reverse rate constants for each subsequent monomer addition step [84]. The authors derived both an exact set of rate equations that must be solved by numerical integration, and an approximate (steady state) set of rate equations for the formation of F-actin (see entry 3 in Table 2). They follow an idea first introduced by Oosawa et al. [77] by distinguishing between the *concentration of polymers* ($c_p = \Sigma\ c_i$) and the *concentration of monomers incorporated into polymers* ($c_p{}^* = \Sigma\ i\ c_i$).

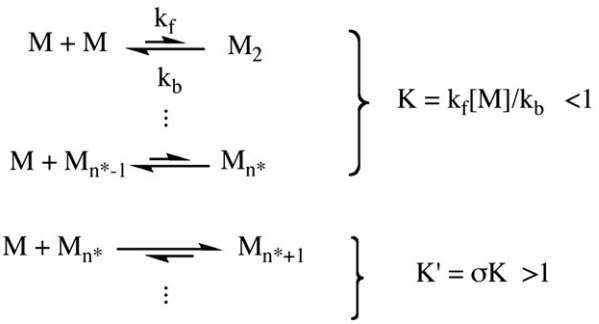

Scheme 3. Hofrichter, Ross and Eaton's nucleation and polymerization mechanism [80]. K indicates a constant with a favorable reverse reaction, while $K' = \sigma K$ indicates a favorable forward reaction.

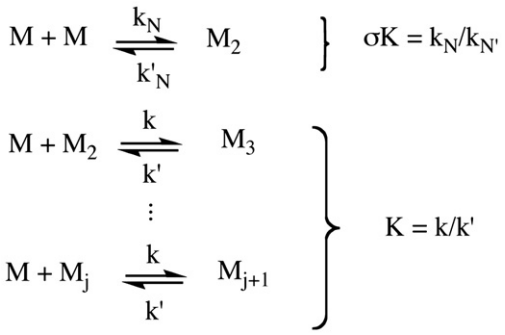

Scheme 4. Wegner and Engel's mechanism for protein aggregation [84].

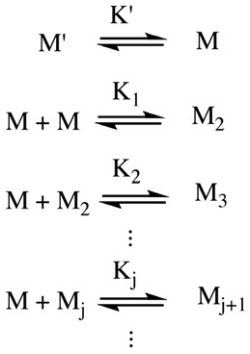

Scheme 5. Frieden and Goddette's mechanism with the added monomer activation step [86].

Also, therein the authors defined the critical nucleus as being "The smallest aggregate for which [the rate of] elongation is faster than [the rate of] dissociation"; in terms of their model, the critical nucleus will be of size $n=2$ if $k[M]>k_N'$, and of size $n=3$ otherwise. They also note that while "Nucleation [is] extremely difficult… cooperativity [is] very high" [84].

An example of Wegner and Engel's kinetic treatment is given in Fig. 4, which shows actin polymerization curves (as measured by light scattering), along with the corresponding calculated kinetic curves. Other researchers have also used Wegner and Engel's polymerization kinetic treatments over the years [85,86].

In 1983, Frieden and Goddette used the subsequent monomer addition model again for protein polymerization, with the exception that each monomer addition step had its own associated equilibrium constant. They also added a step that would occur prior to all the other steps, that of an *activation* of the monomer, as shown in Scheme 5 where M′ is the native monomer, M is the activated monomer, M_n is the polymer of length n, and K_n is the equilibrium constant [86]. The authors proposed that, in the case of actin, the activation step represented a ligand binding to a metal, followed by a conformational change that would accelerate the polymerization process [86]. The authors were able to build upon the work of Wegner and Savko [92] to simplify their system of equations, and used computer simulation tools in their kinetic treatment. Based on their mechanistic analysis they note, "There is no simple measure (i.e., half-time, lag time) which would characterize the rate of polymerization… Thus, it is necessary to fit the full time course of polymerization" [86]. Our own experimental studies confirm this important directive [unpublished results, 163].

Fig. 5 shows polymerization curves of fluorescently labeled actin, along with the computer simulation curves obtained by Frieden and Goddette using an extension of Wegner and Engel's equation (entry 3 of Table 2).

Also in 1983, De Levie et al. applied the subsequent monomer addition mechanism to a series of papers on the nucleation and linear growth of polymers [87,88], in which they used the assumptions that: (i) the active surface area (i.e., the end(s) of the polymer) is independent of particle size; (ii) there is an equilibrium constant for nucleation, and another for growth; (iii) the concentration of nuclei increases with time during the nucleation phase, but remains mostly constant during the growth phase; and (iv) the concentration of monomer is mainly constant at short times. The authors used Laplace transforms and a range of confluent hypergeometric functions to solve the sets of differential equations, both in the case of reversible and irreversible growth. Then using steady-state approximations, they obtained analytical expressions for a *flux in concentration* ($J=d/dt\ \Sigma\ c_i$) and for the *monomer uptake* ($-dM/dt=d/dt\ \Sigma\ i\ c_i$) (see entry 5 in Table 2). However, fits to the proposed equations were not provided [88]. The authors concluded that the sigmoidal ("S") shape of the aggregation curve could be obtained from the growth alone, but that nucleation is necessary to keep the concentration of nuclei at a steady-state value [88]. However, later work [89] shows that *both* nucleation and growth are crucial to obtaining sigmoidal-shaped curves.

In 1986, Goldstein and Stryer added a modification to the subsequent monomer addition mechanism in which, instead of defining the critical nucleus (whose size will depend on the relative rates of elongation and dissociation, and may ultimately depend on monomer concentration, see Hofrichter et al. [80], and Wegner and Engel [84]), they define instead a "seed" s, as "…the length s, where the kinetic constants change" [90]. Thus the equilibrium constant

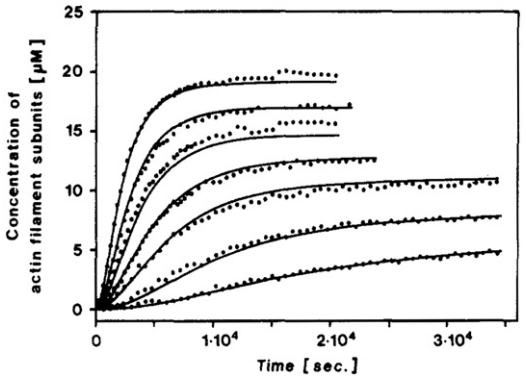

Fig. 4. Wegner and Savko's actin polymerization curves measured by light scattering (dotted lines), along with calculated kinetic curves using the equation shown in entry 3 of Table 2 (solid lines). Reprinted with permission from Ref. [92]. Copyright (1982) American Chemical Society.

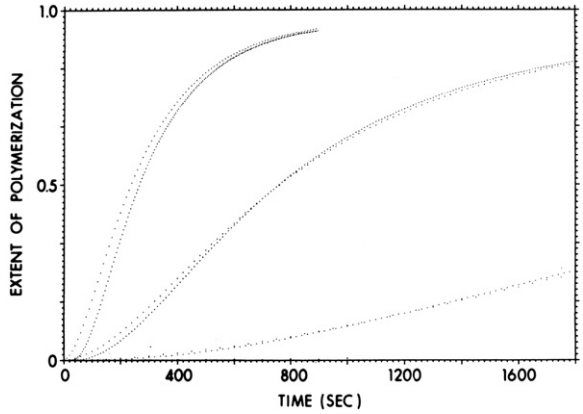

Fig. 5. Fluorescently labeled actin polymerization curves (dotted lines), along with computer simulation curves (solid lines) from Frieden and Goddette. Fig. 7b reprinted with permission from Ref. [86]. Copyright (1983) American Chemical Society.

$$\text{n < seed:}\quad M + M_n \underset{k_-}{\overset{k_+}{\rightleftharpoons}} M_{n+1} \quad \Big\} \; K_a = k_+/k_-$$

$$\text{m ≥ seed:}\quad M + M_m \underset{g_-}{\overset{g_+}{\rightleftharpoons}} M_{m+1} \quad \Big\} \; K_b = g_+/g_-$$

Scheme 6. Goldstein and Stryer's mechanism for protein aggregation [90].

($K_a = k_+/k_-$) is the same for each step prior to the formation of the seed and after the formation of the seed, the equilibrium constant ($K_b = g_+/g_-$) is the same for every subsequent step (see entry 6 of Table 2) [90]. Scheme 6 shows their proposed mechanism where M is the monomer, M_n is a polymer of length n, k_+ and k_- are the forward and reverse rate constants prior to the formation of the seed, and g_+ and g_- are the forward and reverse rate constants after the formation of the seed [90]. The authors aptly note that "The basic equations governing protein polymerization form an infinite interrelated set of differential equations that cannot be solved exactly, and simplifying assumptions must be used" [90]. Also provided in the original reference [90] are simulations of the equations shown in entry 6 of Table 2.

Authors like Oosawa et al. [91] and Wegner and Savko [92], added additional steps of polymer fragmentation (Oosawa and Wegner), displayed with rate constant k_f, and of polymer association (Oosawa), shown with rate constant k_a, to their models of the subsequent monomer addition mechanism, as shown below in Scheme 7.

5.1.2. The reversible association mechanism

Another class of mechanisms involves studies looking at the aggregation of glutamate dehydrogenase, an allosteric enzyme linking the Krebs cycle and amino acid synthesis. Nucleation is usually not accounted for kinetically in these reversible association mechanistic postulates.

Building upon previous studies by Ts'o et al. [93] and by Van Holde and Rossetti [94] for purine association, and using Adams, Jr. and Lewis's 1968 study of β-lactoglobulin self-association [95], in 1970 Eisenberg suggested a reversible association mechanism for the aggregation of glutamate dehydrogenase. This mechanism is shown in Scheme 8 where M is the monomeric species, M_n is the polymerized species of length n, and K is the equilibrium constant that is assumed to be the same for each association step [96].

The use of approximations at low enzyme concentration [95] lead to an estimate of average molecular weights found to be in good agreement with sedimentation experiments (see entry 7 in Table 2) [7,96]. An example of the concentration dependence of these molecular weights, along with calculated curves, is shown in Fig. 6.

Thusius in 1975 and 1976 [8,9,10] challenged the reversible association mechanism put forth by Eisenberg (Scheme 8) [7] for the

$$M + M \underset{}{\overset{K_1}{\rightleftharpoons}} M_2$$
$$\vdots$$
$$M + M_j \underset{}{\overset{K_j}{\rightleftharpoons}} M_{j+1}$$
$$\vdots$$
$$M_j + M_k \xrightarrow{k_a} M_{j+k}$$
$$M_{m+n} \xrightarrow{k_f} M_m + M_n$$

Scheme 7. Subsequent monomer addition mechanism which includes polymer fragmentation and association.

$$M + M_n \overset{K}{\rightleftharpoons} M_{n+1}$$

Scheme 8. Eisenberg's reversible association mechanism [96].

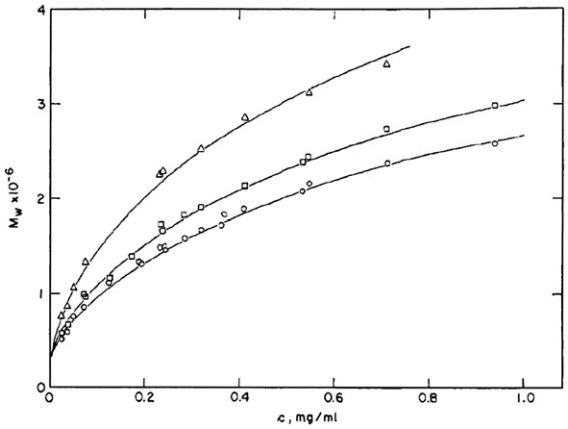

Fig. 6. Average molecular weights of glutamate dehydrogenase measured by light scattering (points), along with calculated concentration dependence curves (line) using the equation shown in entry 7 of Table 2 from Eisenberg. Reprinted with permission from Ref. [7]. Copyright (1971) American Chemical Society.

aggregation of glutamate dehydrogenase. Thusius claimed that the Eisenberg's reversible association mechanism *alone* is not able to account for all the aggregation data in varying concentration ranges [8]. Thusius proposed a variation of the reversible association

$$M_i + M_j \underset{k_d}{\overset{k_a}{\rightleftharpoons}} M_{i+j}$$
$$i, j = 1, 2 \ldots \infty$$

Scheme 9. Thusius' random association mechanism [8].

$$2\,A \underset{k_d}{\overset{k_a}{\rightleftharpoons}} B$$

Scheme 10. A simplified version of the random association mechanism called the "Two-State" mechanism [8].

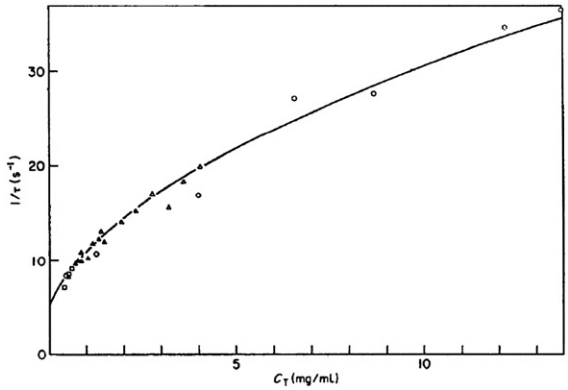

Fig. 7. Thusius's glutamate dehydrogenase reciprocal relaxation times (points), and calculated concentration dependence curve (line) using the equation shown in entry 8 of Table 2. Reprinted from Ref. [9]. Copyright (1975) with permission from Elsevier.

mechanism that they termed the random association mechanism, Scheme 9, in which two (*monomeric* or *polymeric*) units of any size can associate together to form a larger polymer [8].

Since Thusius' mechanism of reversible self-association occurs with "condensation occurring between all species without discrimination" [8], the authors simplified the mechanism by approximating it as a "two-state" mechanism, Scheme 10 [8]. In the "two-state" mechanism, A represents "free association sites", and B represents "bonds between units". The authors note that, "Although [their mechanism] involves more interactions than [the mechanism of sequential monomer addition only], it is the simplest kinetic model… in the sense that all elementary reactions are formally accounted for in a single transformation" [8].

From the simplified "two-state" mechanism, the authors were able to write (and solve) a rate equation for the concentration of "free association sites" A (see entry 8 of Table 2) which they used to test their random association mechanism using light scattering aggregation data [8]. An example of the dependence of relaxation times on concentration, along with a calculated curve, is shown in Fig. 7. The observable data are well fit by the two-state mechanism.

5.1.3. The mechanisms of prion aggregation

The exact, molecular mechanism for the transmission and propagation of prion diseases is generally believed to be intimately linked to the mechanism of aggregation of the prion protein. Many researchers in the area of prion aggregation have, therefore, focused on the molecular details of prion aggregation. Four different mechanisms have been proposed in the literature that provide alternative descriptions of how transmission and propagation of the prion disease may occur through a prion agent. We have chosen to express these mechanisms as chemical reactions rather than pictures or words (as given in some of the original references [4,28]), and have followed Eigen's [97] convention in the choice of arrows used to describe the mechanisms of Prusiner and Lansbury. In Schemes 11–15 below, C represents the cellular form of the prion protein (of predominantly α-helix secondary structure), and P represents the prion form of the protein (which is aggregation prone with a secondary structure of high β-sheet character). The non-prion (i.e., cellular) and prion forms of the prion protein, C and P respectively, are believed to be conformational isomers [4].

In 1967, a mathematician named Griffith proposed three possible theoretical mechanisms that could explain the self-replication of the prion disease agent scrapie [98]. These mechanisms made use of the new hypothesis that the scrapie agent could be a protein, and one is shown in Scheme 11. In Griffith's words, C would be the "stable" form of the protein, and P the "reactive" form. Griffith also proposed that *P be a different conformation of C*. In this mechanism (sometimes referred to as Template Assembly or TA [28]), the conformational change between C and P monomers is thermodynamically unfavorable. Yet if the aggregation of P is thermodynamically favorable enough, it can act as a driving force to promote the overall conversion of two C monomers into a P_2 dimer. Further conversion of C monomers into an aggregated P form is then assisted by the presence of dimers and larger oligomers of P, which act as *templates* [98]. In this mechanism, the infectious species is an oligomer P_x (with $x \geq 2$), and propagation occurs through templated assembly and conversion of C monomers.

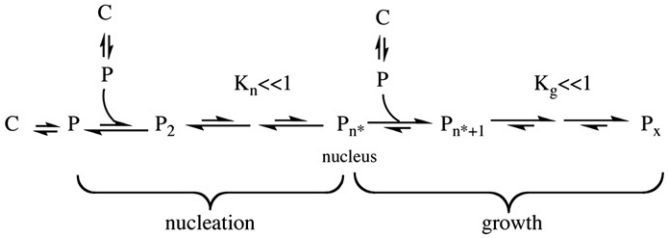

Scheme 13. Lansbury's mechanism for prion aggregation [103].

In 1982, Prusiner presented enough experimental data to support the then controversial idea that the infectious scrapie agent is made of protein, and coined it prion (for *p*roteinaceous *i*nfectious -*on*) [99]. In 1991, he proposed a mechanism of prion transmission and propagation shown in Scheme 12 [4,100] (this mechanism is sometimes referred to as Monomer-Directed Conversion or MDC [28]). In this mechanism, the infectious species is a P monomer that is able to catalyze the otherwise slow conversion of C monomer into P monomer (through the formation of a C•P dimer); propagation thus occurs (we and others [76,97] note) by *autocatalysis* as P is both a reactant and a product of the reaction. Prusiner later acknowledged subsequent aggregation of the infectious form of the protein [101].

In 1996, Eigen published a kinetic analysis of Prusiner's mechanism (see entry 9 in Table 2) [97]. He also provided an alternative version of that mechanism by pointing out that the catalytic (infectious) agent could be either a P monomer (his "linear Prusiner mechanism") or a P_x oligomer (his "cooperative Prusiner mechanism") [97]. Researchers like M. Laurent have provided support for the Eigen's "cooperative Prusiner mechanism" by pointing out that unrealistic rate constants would be needed for P to be the catalytic agent [102].

Following the work of Prusiner, in 1993 Lansbury, Jr. proposed a mechanism of prion transmission and propagation (referred to as Nucleation-Dependent Polymerization, NP), which includes features from the mechanism of subsequent monomer addition discussed above [103–106]. This mechanism is shown in Scheme 13, where n^* represents the critical nucleus size, and K_n and K_g are the equilibrium constants for nucleation and growth, respectively. Here C and P monomers are in equilibrium, and P monomers are slowly

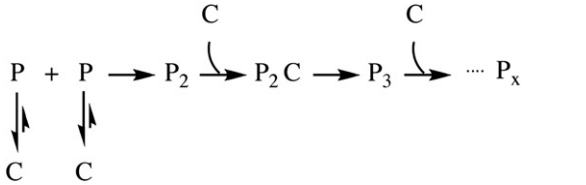

Scheme 11. Griffith's mechanism of scrapie aggregation [98] expressed in more commonly denoted P and C terms.

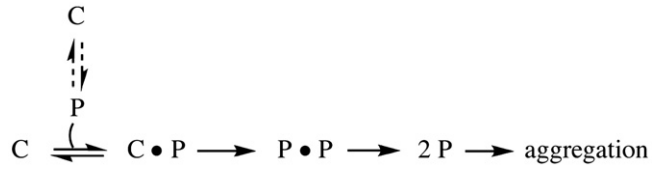

Scheme 12. Prusiner's mechanism for prion aggregation [4] expressed via chemical equations.

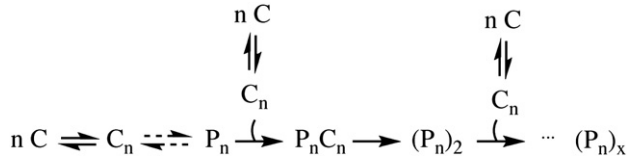

Scheme 14. Lindquist's nucleated conformational conversion mechanism [28] expressed via chemical equations.

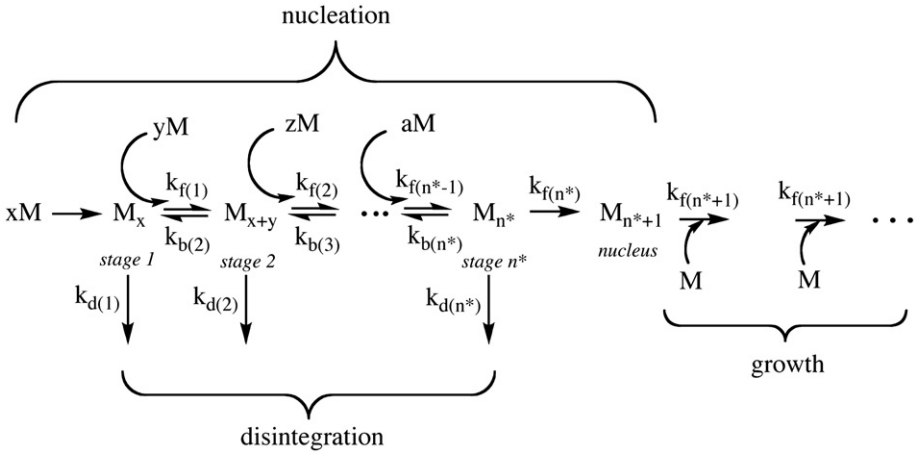

Scheme 15. Flyvbjerg, Jobs, and Leibler's model for the self-assembly of microtubules [108] expressed in terms of chemical equations.

aggregating to form a critical nucleus (nucleation). Once the P_x oligomer is past the critical nucleus size ($x \geq n^*$), further aggregation becomes thermodynamically favorable and leads to growth. In this model, the aggregation of P through *nucleated polymerization* is the driving force that displaces the equilibrium between C and P (towards P) [103]. The infectious species is a seed P_x of size $x \geq n^*$, and propagation occurs through growth on the seed in this model.

In 1996, Eigen also published a kinetic analysis of Lansbury's mechanism (see entry 10 in Table 2) [97]. There he points out is that catalysis *per se* is not necessary in this mechanism (and he defines both a *passive* and an *active* form of autocatalysis,[4] although these terms have not been extensively used in subsequent literature) [97]. Eigen further states that neither the Pruisner nor the Lansbury mechanisms can be ruled out as possible mechanisms of prion transmission and propagation [97].

While studying the aggregation of yeast prion proteins, Linquist proposed a new mechanism in 2000, (which can be seen as a combination of the mechanisms of Griffiith and Lansbury), named Nucleated Conformational Conversion (NCC) and shown in Scheme 14 [28,107]. Here the formation of nuclei of C is followed by slow conversion to nuclei of P. Once nuclei of P are present, further assembly is proposed to occur rapidly. The formation of larger aggregates occurs by *nuclei of P* acting as *templates*, which combine with and convert nuclei of C [28]. In this mechanism, the infectious species is a P nucleus (P_n), and propagation occurs through templated assembly and conversion of C nuclei (C_n).

Attempts have been made in the prion literature to rule out some of the proposed prion mechanisms [28]. However, proper kinetic analyses are lacking [29] particularly because the mechanisms are usually displayed in words and pictures only (a form which is not amenable to rigorous kinetic and associated mathematical analyses).

5.1.4. The subsequent monomer addition mechanism II. Later contributions

In 1996 Flyvbjerg, Jobs, and Leibler examined the self-assembly of microtubules from tubulin using a model described in Scheme 15 where M is the monomer, M_{n^*+1} is the nucleus of size (n^*+1), and k_f, k_b, and k_d are the rate constants for the forward, backward, and disintegration steps, respectively [108].[5] The authors used the assumptions that (i) there is only one pathway for aggregation during nucleation, and (ii) during growth, every stage in the pathway is linked to the next stage by the addition of monomers only [108]. Note that while the steps are reversible up to the formation of the nucleus, they are irreversible thereafter. This model also accounts for the possible disintegration of the intermediate aggregate species during the nucleation phase. The associated rate equations for this model are shown in entry 11 of Table 2.

The authors applied a method of so-called "phenomenological scaling" to a series of kinetic aggregation curves (measured by turbidity at different tubulin concentrations), in which they essentially reduce the data to a common turbidity scale (A/A_∞, where A_∞ represents the maximum turbidity value) and a common time scale (t/t_0, where t_0 represents a "characteristic time" value determined during the scaling process), Fig. 8. By applying their "phenomenological scaling" to variables present in the model's associated rate equations (see entry 11 of Table 2), such as time, monomer concentration, number concentration of monomers, and mass polymerized, the authors were able to find an approximate solution for

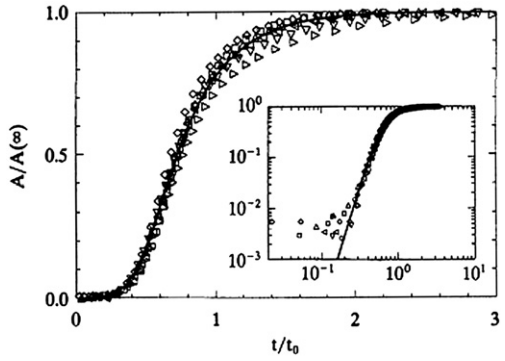

Fig. 8. Flyvbjerg et al.'s microtubule assembly kinetics at various concentrations with the "phenomenological scaling" applied to the data on both the *x*- and *y*-axes. The fit is to the model described in Scheme 15. Note that the inset uses a log–log scale which tends to visually exaggerate the differences in values near zero. Ref [108]. Copyright (1996) National Academy of Sciences, USA.

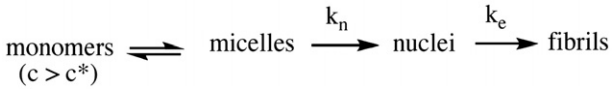

Scheme 16. Word interpretation of Benedek and Teplow's mechanism for protein fibrillation [109].

[4] According to Eigen: "The nucleus may be considered as a 'passive' autocatalyst…[S]uch a process is virtually indistinguishable from any 'active' form of catalysis, that is, a direct interaction of A-particles with some 'catalytic surface' of the B-aggregates." It is not clear whether the distinction of such putative forms of autocatalysis has any physical or chemical basis.

[5] We thank a referee for directing us to this reference.

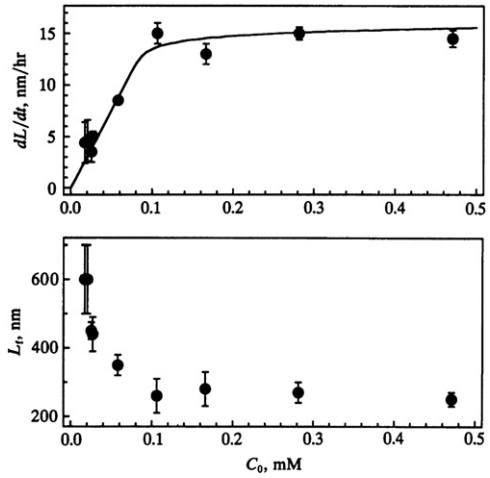

Fig. 9. Benedek and Teplow's concentration dependence on the rate of change in fibril length (dL/dt) and the final fibril length (L_f) observed for amyloid-β with quasi-elastic light scattering. Ref. [109]. Copyright (1996) National Academy of Sciences, USA.

their equation system [108]. Fig. 8 also shows the fit to the proposed model, but which the authors note "was obtained by assuming scaling, a property that is only approximately satisfied by the experimental data" [108].

Flyvbjerg et al. first used four rate constant parameters (from an empirical estimation of the number of assembly steps occurring during nucleation), but found that three of those four rate constants were equivalent, so that their model could be reduced to a two parameter model, which the authors state can be seen as a generalization of Oosawa's classical nucleation-polymerization model. The authors tested this model with turbidity vs. time data for tubulin aggregation at various concentrations, and reported average parameter values of $\prod_{i=0}^{4} k_{f(i)} = (1.2 \pm 0.3) \times 10^3$ cm^{15}/min^5 and $k_{f(1)} = k_{f(2)} = k_{f(3)} = 1.0 \pm 0.9$ cm^3/min. Interestingly, we show that the same data can also be fit with the (phenomenological) 2-step Finke–Watzky (F–W, *vide infra*) model of nucleation and autocatalytic growth (see Fig. S1 of the Supporting information). The averaged rate constants resulting from the F–W fits differ in units from the above results (with $k_1 = (2 \pm 2) \times 10^{-2}$ min^{-1} and $k_2 = 1.7 \pm 0.4$ cm/min), and thus are not directly comparable.

Also in 1996, Benedek et al. looked at the fibrillation of amyloid-β, a peptide whose deposition is associated with Alzheimer's disease, under conditions where the protein is in high concentrations (0.1 mM range), but where the aggregation is slowed down in this case by acidic conditions, so that it may be followed (over time) by quasi-elastic light scattering (QLS) [109]. The authors proposed a model interpreted in Scheme 16, where c represents the protein concentration, c^* the critical micelle concentration (CMC), k_n the rate constant for nucleation, and k_e the rate constant for elongation. In this model and at protein concentrations above the CMC ($c > c^*$), (i) the protein forms micelles, (ii) nucleation occurs within the micelles, and (iii) elongation takes place on the nuclei (by irreversible binding of monomers to the fibrils ends). For protein concentrations below the CMC ($c < c^*$), no nucleation occurs so that (seeded) growth may only take place on impurities [109]. Other researchers have since proposed that soluble oligomers of amyloid-β actually represent protein micelles [110].

The authors emphasized the need to deconvolute kinetic parameters for nucleation *and* growth, as illustrated by the point that an increase in nucleation (*relative* to growth) may both be seen as *promoting* fibrillation (by giving rise to a higher number of fibrils) or as *inhibiting* fibrillation (by leading to shorter fibrils), and vice versa for a decrease in nucleation [109]. From their model the authors derived analytical expressions for quantitative aspects such as the number of fibrils and the final length of fibrils (see entry 12 in Table 2). The authors used these equations to extract rate constants from the observed concentration dependences of L_f, the final length of fibrils, and of dL/dt, the rate of change in fibril length (Fig. 9).

In 1997, the same team published a more detailed mathematical treatment where they relate the measured hydrodynamic radius to a fibril distribution [111]. The authors did so with the use of nth order mathematical moments of fibril distribution: in their treatment, 0th order corresponds to the *sum of fibrils of all sizes* (analogous to the 'concentration of polymers' quantity used by Oosawa [74], *vide supra*), and 1st order corresponds to the *sum of all protein in fibril form* (again, see the 'concentration of monomers in polymers' quantity used by

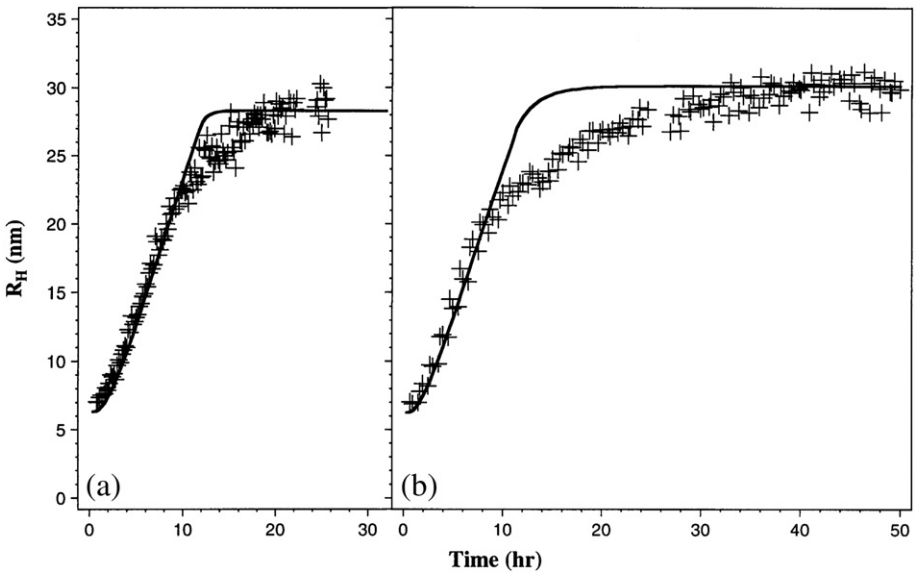

Fig. 10. Amyloid-β aggregation followed by quasi-elastic light scattering: hydrodynamic radius (R_H) as a function of time, along with calculated curves from Benedek et al. Ref. [111]. Copyright (1997) National Academy of Sciences, USA.

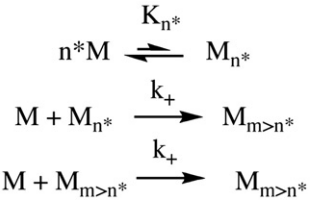

Scheme 17. Ferrone's proposed mechanism as interpreted as part of the present work.

Oosawa [74] *vide supra*) [111]. Fig. 10 shows the evolution of the measured hydrodynamic radius, R_H, as a function of time, along with calculated curves. This work represents an early and detailed effort at expressing aggregate size as a function of time, a problem more recently investigated by R. M. Murphy and M. M. Pallitto [112].

In 1999, Ferrone published a paper on the kinetics of protein aggregation in which he used a mechanism of subsequent monomer addition analogous to the one described in Scheme 3 above, where he defines the critical nucleus as the aggregate size after which "the association rate exceeds the dissociation rate for the first time" [113]. With assumptions similar to those made by De Levie in 1983 [88], but using a perturbation theory approach instead [114], the author derived an expression for the monomer concentration as a function of time (see entry 13 in Table 2) [113]. Ferrone's expression turns out to be mathematically identical to that obtained by De Levie in the case of irreversible growth [88] (see entry 5 in Table 2); for a detailed analysis of the equivalence between De Levie and Ferrone's expressions, see Scheme S1 of the Supporting information. The author also made use of the distinction employed by Oosawa [78] (*vide supra*) between the concentration of *polymers* and that of *monomers incorporated into polymers* [113].

Shown in Scheme 17 is our translation of Ferrone's equations [113] into chemical reactions, where M represents the protein monomer, M_{n^*} the nucleus of size n^*, $M_{m>n^*}$ any polymer of size $m>n^*$, K_{n^*} is the nucleation equilibrium constant, and k_+ the rate constant for growth.

Using our interpretated scheme of Ferrone's mechanism along with the assumptions employed in his treatment [113], we have also attempted to express the corresponding rate equations in Eq. (1). The assumptions Ferrone used that we have also employed in attaining Eqs. 1(a)–1(c) are that: (i) all polymers can be counted by their ends *only* (so that they appear unchanged on both sides of the reaction, see the third step in Scheme 17); (ii) the concentration of nuclei is *small* (so that the monomer uptake occurs mostly through the growth of polymers, see Eq. 1(c)); and (iii) initially, the concentration of monomers incorporated into polymers is *very small* compared to the initial monomer concentration (in the first 10–15% of the aggregation curve), so that there the concentration of free monomer can be assumed to be constant and equal to the initial value (and the rate Eq. (1.a,b,c) can be integrated using a constant term $[M]=[M]_0$) [113]. The resulting equations are:

$$\text{(a)}\quad \left[M_{n^*}\right] = K_{n^*}[M]^{n^*}$$

$$\text{(b)}\quad \frac{d\left[M_{m>n^*}\right]}{dt} = k_+[M]\left[M_{n^*}\right] \qquad (1)$$

$$\text{(c)}\quad -\frac{d[M]}{dt} = k_+[M]\left[M_{mNn^*}\right]$$

In 2002, Wetzel applied Ferrone's equation to the aggregation of polyglutamine [115,116], as shown in Eq. 2 below, where Δ is the concentration of polymerized monomer, c_0 is the initial concentration of monomer, c is the concentration of free monomer, k_+ is the second-order elongation rate constant, K_{n^*} is the nucleation equilibrium constant, and n^* is the critical nucleus.

$$\Delta_{(t)} = c_0 - c_{(t)} = \frac{1}{2}k_+^2 K_{n^*} c^{(n^*+2)} t^2 \qquad (2)$$

The use of eq. 2 is limited to the early portion of the kinetic curve [25], where the concentration of monomer may be taken as constant and equal to the initial value. In the early portion of the curve (≤15% of the aggregation curve), a plot of $\{\Delta_{(t)}$ *vs.* $t^2\}$, as in Fig. 11, gives a slope of $[1/2\ k_+^2\ K_{n^*} c^{(n^*+2)}]$; in turn a plot of {ln(slope) *vs.* ln(c_0)} gives $[(n^*+2)]$ as a slope and $[\ln(1/2\ k_+^2\ K_{n^*})]$ as an intercept [117]. This formula has been used to extract information about the critical nucleus size [115–118,], but it should be noted that nucleation and growth are still convoluted in the intercept.

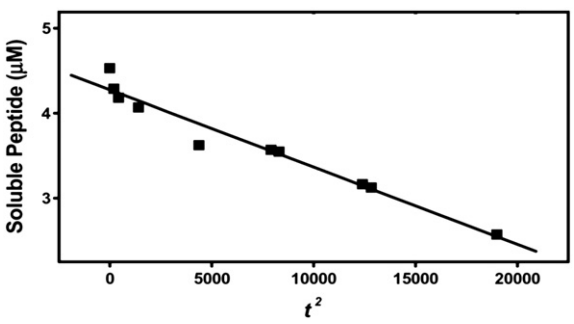

Fig. 11. An example of Ferrone and Wetzel's soluble monomer concentration vs. t^2 plot for the early portion of the aggregation curve of polyglutamine fit using Eq. 2. Fig. 2d of Fig. 2a–d reproduced from Ref. [115]. Copyright (2002) National Academy of Sciences, USA.

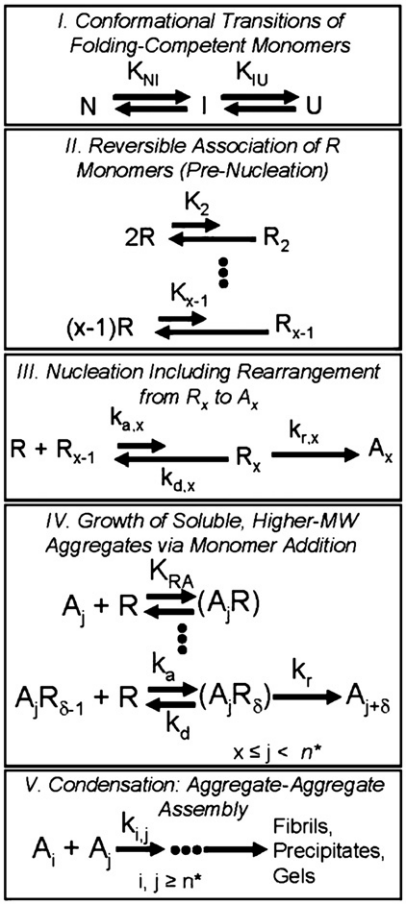

Scheme 18. Roberts' nucleated polymerization mechanism. reprinted with permission from Ref. [120]. Copyright (2007) American Chemical Society.

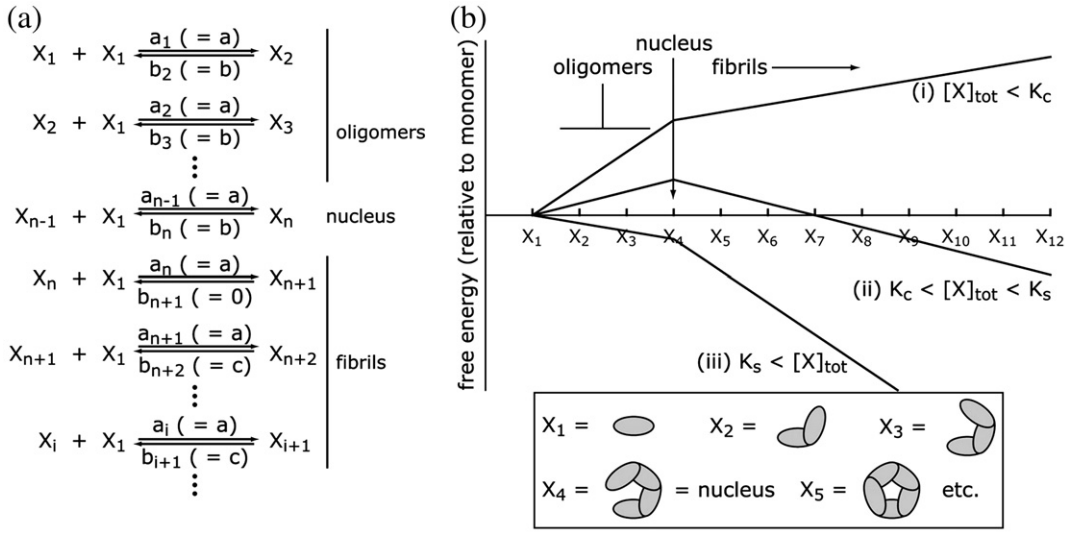

Fig. 12. Three kinetic regimes proposed by Powers and Powers for the mechanism of subsequent monomer addition. Reprinted with permission from Ref. [125]. Copyright (2006) Biophysical Society.

In 2003, while exploring ways to predict a protein shelf-life, Roberts proposed a mathematical model for the irreversible aggregation of proteins in which the final product is amorphous aggregates [11]. In his approach, Roberts used an extended Lumry–Eyring model [119] to account for protein denaturation prior to aggregation. In 2007, Roberts adapted his model to the aggregation of proteins for which the final product of aggregation is ordered aggregates (i.e., fibrils) [120]. He proposed a mechanism reproduced in Scheme 18 (also see entry 14 in Table 2) [14,121]. In stage I (which corresponds to conformational changes involving the monomer), N represents a monomer in its native state, I in its intermediate state, and U in its unfolded state, while K_{NI} and K_{IU} are equilibrium constants for $N \rightleftharpoons I$ and $I \rightleftharpoons U$, respectively. In stage II (which is a "pre-nucleation" stage of reversible monomer association), R represents the reactive form of the monomer (N, I or U), R_i a reversible oligomer (composed of i monomers), and K_i is the equilibrium constant for $iR \rightleftharpoons R_i$. In stage III (which corresponds to nucleation involving a rearrangement), A_x represents the aggregate nucleus, x the nucleus size, and $k_{a,x}$, $k_{d,x}$, and $k_{r,x}$ are the association, dissociation, and rearrangement rate constants, respectively, for the nucleation step. In stage IV (in which the soluble aggregates grow through monomer addition), A_j represents an aggregate composed of j monomers, A_jR the reversibly associated A_j and R, K_{RA} is the equilibrium constant, and δ is the number of monomers in each growth event. In stage V (where the condensation of aggregates leads to the formation of say, fibrils), n^* represents the size at which condensation begins, and k_{ij} is the rate constant for the condensation of $A_i + A_j$.

In this model, the protein aggregates are in a non-native (reactive) state, and Roberts has since proposed a version of this model for aggregation of protein in its native state (where stages I, III and V are omitted) [14]. The authors introduce and examine several kinetic regimes that are defined by the relative rates of nucleation and growth, and by the size at which the aggregates condense [120]. Simulations predict that these kinetic regimes should be differentiable experimentally by a combination of (i) apparent reaction order; (ii) dependence on the initial protein concentration; and (iii) aggregate size distribution [120]. Roberts also states that his model has the ability to encompass (most) previously proposed models, as these can be classified based on which stages they do include and where the rate limiting step occurs [14]. We agree that Roberts' model is able to account for many of the previous models for protein aggregation; however, application of this model to experimental protein aggregation data is not a simple task, but has been reported [122,123,124].

In 2006 Powers and Powers, while looking at the kinetics of subsequent monomer addition, proposed that three distinct regimes exist based on the total protein concentration: (i) low, (ii) medium and (iii) high [125]. The concentration "cut-offs" for these regimes are determined by the values of $K_{c(\text{critical})}$, the equilibrium constant for monomer dissociation *subsequent* to the formation of a (structural [125]) nucleus and $K_{s(\text{supercritical})}$, the equilibrium constant for monomer dissociation *prior* to the formation of that nucleus, see Fig. 12.

(i) In the low regime, defined for total protein concentrations lower than K_c, all the polymers (including oligomers, *structural* nucleus [125] and fibrils) are higher in energy than the monomer, and as a consequence no fibrillation occurs. (ii) In the medium regime, defined for protein concentrations larger than K_c but less than K_s, the highest energy species is the structural nucleus [125], and fibril formation occurs through a (classic) nucleated polymerization pathway. (iii) In the high regime though, defined for protein concentrations larger than K_s, the highest energy species is now the monomer, and the authors warn that (classic) models of nucleated polymerization may no longer apply [125]. The authors test their proposed mechanism with *simulations* using various concentrations. The simulations are consistent with the above three regime model, although no experimental kinetic data were used [125]. Recently, Powers and Powers have added off-pathway aggregation to their mechanism and tested this updated model again using simulations, but this time with more experimentally relevant concentrations [56].

5.1.5. An "Ockham's razor"/minimalistic 2-step model

This class of kinetic mechanisms for particle aggregation was first proposed in 1997 by Finke and Watzky for transition-metal nanocluster formation [89], but was recently shown to apply to a broad spectrum of aggregating proteins, including α-synuclein, amyloid-β, polyglutamine and prions, relevant in the neurodegenerative disorders of Parkinson's, Alzheimer's, Huntington's and prion diseases, respectively (entry 15 of Table 2) [29,76]. In Scheme 19 below and in

$$A \xrightarrow{k_1} B$$
$$A + B \xrightarrow{k_2} 2B$$

Scheme 19. The Finke–Watzky (F–W) mechanism [89] that has been applied to 41 literature protein aggregation data sets [29,76].

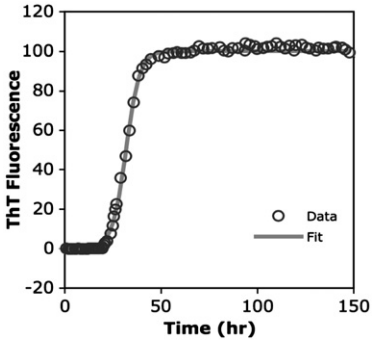

Fig. 13. An example of aggregation data published by A. L. Fink [37] and fit to the F–W 2-step mechanism. In this case, aggregation of α-synuclein in the presence of macromolecular crowding was measured by fluorescence [37] data were digitized and fit to the F–W mechanism resulting in $k_1 = 4.0(8) \times 10^{-5}$ h^{-1}, $k_2 = 4.0(1) \times 10^{-3}$ μM^{-1} h^{-1}, and a coefficient of determination (R^2) of 0.999. Reprinted with permission from Ref. [76]. Copyright (2008) American Chemical Society.

the case of protein aggregation, A represents a (precatalytic) form of the protein monomer while B represents any (catalytic) aggregated form of the protein past the critical nucleus size. Hence, all aggregates able to perform autocatalysis are treated as kinetically equivalent species in this minimalistic kinetic model. Importantly, the rate constants k_1 and k_2 correspond to nucleation and growth, respectively, so that this two-step model specifically and easily separates (average) nucleation from (average) growth. Also, as the species B is both a catalyst and a product in the growth step reaction, the latter step is the definition of autocatalysis (A+B→2B being the elementary step that defines autocatalysis).[6]

As shown in Scheme 19, the F–W model consists of two simple *pseudoelementary* steps.[7] By definition a pseudoelementary step can be employed *kinetically* as an elementary step, and as such its rate law can be determined from the stoichiometry of the reaction. Within the F–W model, all the probably hundreds to thousands of actual steps occurring at the molecular level of the aggregation process can be combined into two pseudoelementary steps [89], as demonstrated by the fact that these two steps alone are able to account for a whole range of protein aggregation kinetic data [29,76]. The two pseudoelementary steps in the F–W mechanism represent respectively, typically slow nucleation and typically fast autocatalytic growth [89]. The rate constants, k_1 and k_2, are *average and pseudoelementary* rate constants for those nucleation and growth steps.

$$n_0A \text{ (monomers)} \overset{K}{\rightleftharpoons} A_{n0} \text{ (micelle)}$$

$$A_{n0} \xrightarrow{k_1} B_{n0}$$

$$A + B_n \xrightarrow{k_2} B_{n+1}$$

Scheme 20. Saitô and co-workers' mechanism for the aggregation of human calcitonin [127].

The F–W 2-step mechanism is an "Ockham's razor," [126] minimal kinetic model, *the first model in which quantitative rate constants for nucleation and growth can be routinely and easily obtained* using either of the analytic equations shown in entry 15 of Table 2 and corresponding to the model in Scheme 19 [89]. An example of a F–W fit previously obtained [76] for the aggregation of α-synuclein [37] is shown in Fig. 13; it is apparent that this simple 2-step mechanism is capable of accounting for the aggregation data. Fits to the aggregation kinetic data from polyglutamine, amyloid-β, prion, and other α-synuclein aggregation have been published, with each of the 41 data sets analyzed showing good to excellent fits to the F–W 2-step model [29,76].

However, due primarily to its minimal simplicity, the F–W mechanism does have limitations, including: (i) hundreds if not thousands of steps are condensed into two pseudo-elementary steps, (ii) the rate constants, k_1 and k_2, are average rate constants, (iii) a higher kinetic order in [A] may be hidden kinetically in the nucleation step in particular, and (iv) all growing aggregates are hidden behind the descriptor 'B' which describes a catalytically active form of "polymerized monomer", the latter concept having been originally introduced by Oosawa [78] and subsequently used by others [84,113]. Recently, we have found that the general descriptor 'B' can also hide processes such as fragmentation [29], which is a topic of future studies [unpublished results]. These limitations have been previously discussed in detail [29,76] for the interested reader.

In 2000, Saitô et al. published a paper analyzing the aggregation of human calcitonin with the mechanism shown in Scheme 20, where n_0 represents micelles of the same aggregation number, A_{n0} is the micelle of n_0 monomers, B_{n0} is the nucleus, and B_n and B_{n+1} are the elongated fibrils with n and $n+1$ molecules of the protein [127]. The concept of (protein) micelle formation [110] during the nucleation phase, invoked in this mechanism, is built upon the work

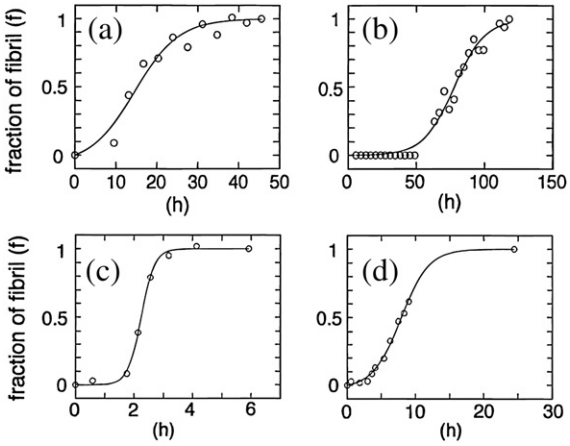

Fig. 14. Saitô's fraction of fibril vs. time human calcitonin aggregation data measured using amino acid labeled solid-state ^{13}C-NMR (A and B) or circular dichroism (C and D, where C is the protein at 1.5 mg/mL and D is the protein at 0.2 mg/mL). The aggregation data was fit using Saitô's fractional equation shown in entry 16 of Table 2. Reprinted with permission from Ref. [127]. Copyright (2000) Cold Spring Harbor Laboratory Press.

[6] The Finke–Watzky (F–W) mechanism can for reasons of visual clarity be expressed in a more descriptive form as shown below, where A again represents the precatalytic form of the protein monomer, and now it is B_n that represents the catalytic form of the aggregated protein. The observed kinetics of the descriptive form would still obey the rate laws of the steps as written in Scheme 18, *during the initial phase of the reaction (i.e., as $t \rightarrow 0$)* where the concentration of monomer A is approximately constant (i.e., $k_{1\ (obs)} \approx k \times K^{n-1} \times [A]_0^{n-1} \approx$ constant, where K is the equilibrium constant for any (reversible) bimolecular association step prior to formation of the nucleus, k is the rate constant for the last (irreversible) bimolecular association step leading to formation of the nucleus, and $[A]_0$ is the initial monomer concentration). However, as t becomes larger, the rate laws and their solutions will deviate (e.g., in the simple case of bimolecular nucleation, when $\frac{-d[A]}{dt} = k[A]^2$ is approximated to $\frac{-d[A]}{dt} \approx k[A]_0[A]$, the solution to the first equation, $[A]_t = \frac{[A]_0}{1 + k[A]_0 t}$, is only equal to the solution of the second equation, $[A]_t = [A]_0 \times e^{-k[A]_0 t}$, if $t \rightarrow 0$, as they both approximate through a Taylor series to $[A]_t = [A]_0(1 - k[A]_0 t)$.) We thank a referee for the specific and useful comments that lead us to clarify this footnote.

$$nA \rightarrow B_nA + B_n \rightarrow B_{n+1}$$

[7] The concept of pseudoelementary steps was introduced in the 1970s by Noyes, who developed this concept using kinetic studies of complex oscillating reactions (J. Am. Chem. Soc. 1972, 94, 8649-8664.; J. Chem. Phys. 1974, 60, 1877-1884.; Acc. Chem. Res. 1977, 10, 214-221.).

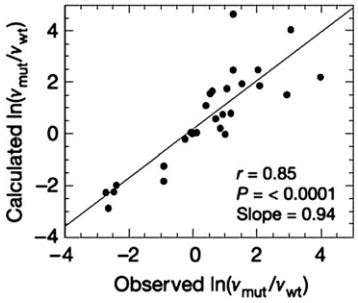

Fig. 15. Chiti et al. calculated and observed changes in the aggregation rate upon a single mutation of 27 proteins data sets including the proteins amylin, amyloid β, α-synuclein, and tau. Fig. 2a of Fig. 2a–b reprinted with permission from Ref. [135]. Copyright (2003) Nature Publishing Group.

of Benedek et al. [109], see Scheme 16. Also published was a resultant differentiated equation shown in entry 16 of Table 2 [127].

Although not readily apparent, the differential equation shown in entry 16 of Table 2 is mathematically identical to the differential equation expressed in terms of $[B]_t$ for the F–W mechanism (entry 15 of Table 2); the analysis of this equivalence can be found in Scheme S2 of the Supporting information in reference [76]. Sample fits using Saitô's fractional equation (entry 16 of Table 2) of human calcitonin aggregation data measured by amino acid labeled solid-state ^{13}C NMR and circular dichroism at two different concentrations of protein are shown in Fig. 14.

Although Saitô's 2000 mechanism is equivalent to the earlier F–W mechanism, Saitô was the first to use the equation shown in entry 16 of Table 2 to analyze the aggregation of proteins (Fig. 14). Other research groups have subsequently used Saitô's fractional form of the F–W equation to fit other protein aggregation kinetic data [128–133].[8]

Later in 2006, Murphy and Gibson published a "two-step kinetic model of aggregation" for the protein insulin, along with its corresponding integrated rate equation (see entry 17 of Table 2) [134]. The integrated rate equation given by Murphy and co-workers in 2006 is equivalent to the integrated rate equation in the 1997 F–W and 2000 Saitô models.

5.1.6. Quantitative structure–activity relationship models

A phenomenological approach to protein aggregation that uses the protein physicochemical properties, was originally developed by Chiti et al., in which they looked at the effect of amino acid mutations on protein aggregation rates. Their approach is to correlate the observed aggregation rate changes to calculated changes in protein physicochemical properties such as hydrophobicity, charge, and propensity to convert from a α-helical to a β-sheet secondary structure [135]. The coefficients for the equation shown in entry 18 of Table 2 are determined by standard regression to fit the observed $\ln(\upsilon_{mut}/\upsilon_{wt})$ values that were obtained using experimental data from the literature (υ_{mut} and υ_{wt} represent the aggregation rates of the mutant and wild-type protein, respectively). It was shown that the hydrophobicity and hydrophobic/hydrophilic patterns (or the propensity to convert from α-helix to β-sheet) contributed positively to the aggregation rate (A, $B>0$), while charge contributed negatively ($C<0$), see entry 18 of Table 2 [135]. As shown in Fig. 15, the authors tested their model using 27 single mutation data sets and compared their calculated $\ln(\upsilon_{mut}/\upsilon_{wt})$ values to the observed $\ln(\upsilon_{mut}/\upsilon_{wt})$ values; they found that their model predicted the observed values with a modest correlation coefficient (r) of 0.85.

Later, Chiti et al. expressed an absolute protein aggregation rate (k) in terms of a combination of physicochemical factors intrinsic and extrinsic to the protein, as shown in entry 19 of Table 2 [136]. This second equation (shown in entry 19 of Table 2) in principle allows the rate of aggregation of the protein to be determined without the need for the mutant aggregation data. Here again the coefficients of the equation are determined by a standard regression of the observed $\log(k)$ values. The authors found here, too, that both hydrophobicity and propensity to convert from α-helix to β-sheet (or hydrophobic/hydrophilic patterns) contributed positively to the aggregation rate (α_1, $\alpha_2>0$), while charge contributed negatively ($\alpha_3<0$), see entry 19 of Table 2 [136]. As shown in Fig. 16 below, the authors tested their equation using 79 data sets; comparison of the calculated $\log(k)$ vs. the experimental $\log(k)$ showed a strong correlation with $r=0.92$.

Although Dobson and co-workers' equations provide a powerful example of a phenomenological approach in which the rate of protein aggregation can be determined, the rate constants obtained from Dobson's equations still contain a *convolution of nucleation and growth* [unpublished results]. Restated, it would be of considerable interest to use Dobson and co-workers' approach, but on separate nucleation and growth rate constants such as k_1 and k_2 of the F-W 2-step model.

5.2. A closer look at the five classes of mechanisms using the concept of polymerized monomer

The concept of polymerized monomer, first introduced by Oosawa [78] and subsequently used by others [84,113], can be used as an approximation tool to encompass *all monomer polymerized into aggregates of different sizes* (with the distinction, for example, of aggregates only past the critical nucleus), into one unique *polymerized monomer* species. This approximation can greatly reduce the complexity of the associated rate equations. For example, using the polymerized monomer approximation allows the mechanism of subsequent monomer addition to be rewritten as in Scheme 21 below, where M represents the protein monomer, P represents *polymerized monomer past the critical nucleus size*, and n represents the critical nucleus size.

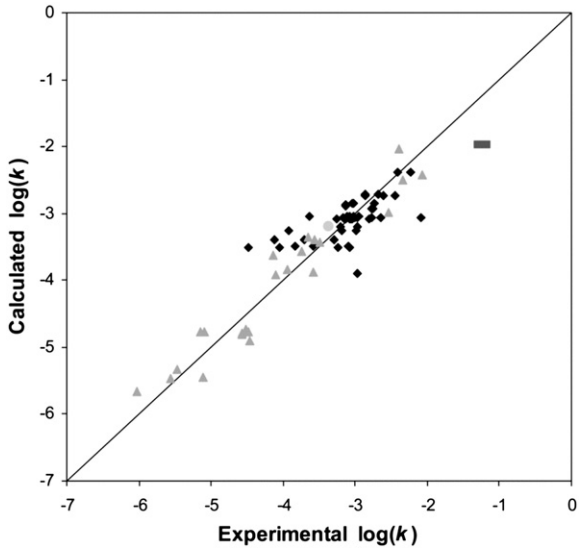

Fig. 16. Calculated and experimentally observed changes in the absolute rate of aggregation (k) for 79 protein aggregation data sets including 59 data sets of WT and mutant human muscle acylphosphatase from Chiti, Dobson and Vendruscolo. Reprinted from Ref. [136]. Copyright (2004) with permission from Elsevier.

[8] The mechanism displayed in Scheme 19 and corresponding equation in entry 16 of Table 2 are original works of Saitô and co-workers in 2000. Although Saitô's work has been properly referenced by some investigators [128,129], it has also been miscited by other investigators [130]. In one unfortunate case, other authors stated that they used a modification when in fact they used the same mathematics originally given by Saitô [130]. This emphasizes a point in the Problem Areas section (vide infra) that knowing the prior protein aggregation literature is necessary and key to avoiding repetition and miscitation.

$$\begin{aligned} nM &\rightleftharpoons nP \\ M + P &\rightleftharpoons 2P \end{aligned}$$

Scheme 21. The subsequent monomer addition mechanism incorporating the polymerized monomer concept, with a critical nucleus size of n.

In another example, the prion mechanisms of Griffith and Lansbury can be rewritten as in Scheme 22 below, where M_c is the cellular prion monomer, M_p is the infectious prion monomer, and P is now the *polymerized infectious prion monomer*. We did not include herein the prion mechanisms of Prusiner, as it did not originally involve aggregation steps, or Lindquist, as that mechanism is not easily simplified by the use of the polymerized monomer concept. Similarly, the reversible association mechanism cannot be rewritten and simplified with *P*.

The F–W mechanism already employs the polymerized monomer concept. Rewriting this mechanism in terms of the nomenclature used above results in Scheme 23, where *M* represents the protein monomer, and *P* represents the *catalytically active polymerized monomer*.

Using the polymerized monomer approximation with the subsequent monomer addition mechanism along with Griffith's and Lansbury's prion mechanisms allows for simplification. In the case of the subsequent monomer addition mechanism (Scheme 21), the polymerized monomer approximation simplifies this mechanism in such a way that it resembles the minimalistic F–W mechanism (Scheme 23).

5.3. Empirical approaches to determine empirical constants of protein aggregation

Empirically based equations are a different approach than those reported in the previous section (and shown in Table 2) to examine protein aggregation kinetic data. Empirical equations typically provide a convenient and easy way to fit the kinetic data of protein aggregation, but they have a significant weakness: there is little or no physical meaning behind the typical empirical equation and, hence, its variables. As such, empirical approaches typically have not provided mechanistic insight into the aggregation process. However, primarily for the sake of completeness, some empirical methods are examined briefly.

5.3.1. Logistic functions

Naiki and co-workers, who developed a first-order kinetic model for the growth only of amyloid-β fibrils (see Table S1 of the Supporting information), also noticed that the sigmoidal aggregation curve obtained by incubation of an amyloid-β monomer, obeys a *logistic function* [137,138,139]. Cerny points out that logistic curves have indeed been shown to empirically fit a wide variety of sigmoidal data [140]. However, to our knowledge, no mechanistic insight has typically come out of fitting protein aggregation data with a logistic function.

Fink et al. have used a modified version [142] of Richards' function to fit sigmoidal aggregation curves observed in the fibrillation of proteins [34,37,141]. Richards' function is itself a generalized form of the logistic function [143], and is commonly used in botany to determine both the growth period length and the ultimate weight of plants [144]. The logistic equation used by Fink and co-workers is shown in Eq. 3 below, where Y is the fluorescence intensity used to measure the aggregation, (y_i+m_ix) is the initial slope during the lag phase, (y_f+m_fx) is the final slope after growth has ended, x_0 is the time at 50% intensity, and $1/\tau$ is the length of time for the lag phase. The lag phase is calculated as $(x_0\times 2\tau)$ and the apparent rate constant k_{app} is $(1/\tau)$ [34].

$$Y = (y_i + m_i x) + \frac{(y_f + m_f x)}{1 + e^{-\left(\frac{x-x_0}{\tau}\right)}} \tag{3}$$

The authors are careful to note that, "This expression is unrelated to the underlying molecular events, but provides a convenient method for comparison of the kinetics of fibrillation" [37]. Fink's empirical equation has been used to analyze numerous data sets thus allowing for comparisons to be made between related data sets [34,35,37,142]; an example is shown in Fig. 17. Again, however, meaningful kinetic and mechanistic information is lacking. Recent work shows that Fink and co-workers' expert biophysical studies and resultant kinetic data can be analyzed by the F–W 2-step model [163].

Recently, McRae and co-workers were able to express the empirical parameters in Fink's logistic equation in terms of kinetic variables from their model [145]. The resulting correlations are complicated, and show that each of these empirical parameters is a convolution of variables such as initial monomer concentration, nucleation, elongation and dissociation rate constants, and average number of monomers per fibril [145]. Again, it would be of use to reanalyze this data in terms of models able to deconvolute average nucleation from average growth [89].

6. Three problem areas in the protein aggregation kinetic and mechanistic literature

One must ask, why has such an important question, as 'what are the mechanism(s) of protein aggregation?', yet to be unequivocally answered despite the numerous contributions cited herein? The simple answer is that protein aggregation is a highly complex problem with complicated molecular level and kinetic details, along with associated complex mathematics. In hopes of moving this area

(a)

$$\begin{aligned} M_c &\rightleftharpoons M_p \\ 2M_p &\rightarrow 2P \\ M_c + P &\rightarrow M_c{\bullet}P \rightarrow 2P \end{aligned}$$

(b)

$$\begin{aligned} M_c &\rightleftharpoons M_p \\ nM_p &\rightleftharpoons nP \\ M_p + P &\rightarrow 2P \end{aligned}$$

Scheme 22. (a) Griffith's and (b) Lansbury's prion mechanisms rewritten with the incorporation of the polymerized monomer concept.

$$\begin{aligned} M &\rightarrow P \\ M + P &\rightarrow 2P \end{aligned}$$

Scheme 23. F–W mechanism rewritten in terms of monomer, M, and polymerized monomer, P.

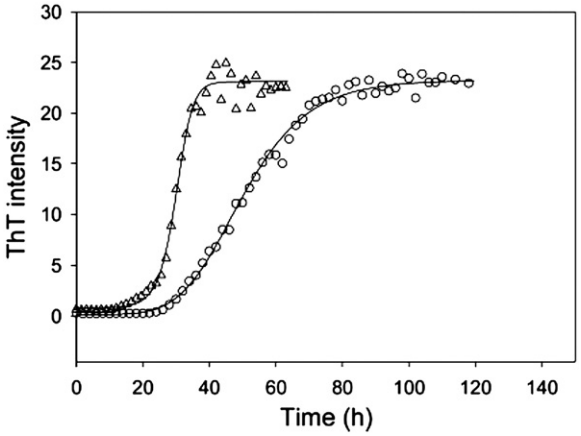

Fig. 17. Aggregation of wild-type and mutant (Y39W) α-synuclein from Fink et al. measured by ThT fluorescence (points), along with corresponding fits using Eq. 3 (lines). Fig. 1b of Fig. 1a–b reprinted with permission from Ref. [36]. Copyright (2006) American Chemical Society.

forward, we list a few possible problem areas of importance, in our opinion, for future studies in protein aggregation.

6.1. Lack of a full appreciation of the previous literature

A complete understanding of the literature in any area is a very important and early requirement for the best and most efficient science—and especially in areas where a large literature exists such as in protein aggregation. However, and unfortunately, constructing this review makes apparent that not all papers published in the protein aggregation area have a clear and comprehensive understanding of the previous literature. Some mechanisms may be proposed only for a specific system of study, with little generalization to try to tie together a broad spectrum of protein aggregation literature. Relevant here is Platt's definition of good science as building upon others' ideas via the disproof of all possible alternative hypotheses [146]. We hope that the present review will help alleviate this problem somewhat—we also offer our sincere apologies to any authors whose crucial literature we have inadvertently overlooked as we strove to distill the protein aggregation literature to its essential components.

6.2. Confused nomenclature

One problem in the area of protein aggregation is that numerous terms are used for identical meanings. An example is with the multiple terms used for growth that include polymerization, elongation, fibrillation and maybe "heterogeneous nucleation"[2] [83]. Also, terms such as "extreme autocatalysis" due to the observation that "the first 10% of the reaction proceeds as the 10th to 20th power of time" [83] are confusing. Note that if one views "heterogeneous nucleation" as "seeded autocatalytic growth, then terms such as "extreme catalysis" are taken care of by autocatalysis. In addition, it is not clear whether the descriptive terms "passive" vs. "active" autocatalysis [97] have any physical or chemical basis.[4] Also used alternately but with identical meaning (to our knowledge), are the terms "positive [kinetic] cooperativity," "positive feedback activation" [147], and "autocatalysis." Many other examples exist, so that we find a need for a clear, unified nomenclature in the area of protein aggregation. The early footnotes herein on nomenclature[1,2] are offered as an aid towards a more unified nomenclature in the protein aggregation area.

6.3. Using word- or picture-only mechanisms

At times, a word or picture-only mechanism may be useful to describe what would account to a very complex set of equations (that may not be tested or even testable due to their associated mathematical complexity). But, as such they do not lead to precise kinetic equations and corresponding differential equations (and then, ideally, their integrated versions), such kinetic equations being required to test the mechanism vs. experimental kinetic data. Another serious issue arises when a word or picture-only mechanism is proposed along with equation(s) that cannot be derived from that (word or picture) mechanism: *a disconnect then results between the mechanism proposed and the equation(s) given*. This is turn leads to the use of at least rigorously undefined, if not the wrong, words for the physical phenomenon at hand. In rigorous mechanistic studies, balanced chemical equations define *both the rate constant* and the *word concepts* that one can use. This is a fundamental, central and important point for proceeding more efficiently in the area of protein aggregation kinetics and mechanism.

7. Summary and conclusions

Despite the importance of the problem and the nearly 50 years of research aimed at determining the mechanism(s) and rate constant(s) for protein aggregation, many questions still remain. Frieden concisely summarizes the state of affairs in his recent review: "In spite of the extensive literature, however, the mechanism of [protein] aggregation is poorly understood" [16]. The focus of the present review has been to examine the protein aggregation literature from the perspective of trying to fit the available protein aggregation kinetic data to obtain quantitative useful rate constants and mechanistic information on the aggregation process. The main contributions from this review are believed to be the following:

- We have briefly reviewed the methods used in the literature to follow protein aggregation pointing out those methods that are direct vs. indirect, and in-situ vs. ex-situ. We have emphasized that the use of multiple techniques is advisable if not necessary to avoid over-interpretation and to ensure that accurate kinetic data are collected.
- We then reviewed what is known about the starting proteins, products, and intermediates of protein aggregation since knowing the products is a necessary prerequisite to reliable kinetic and mechanistic work. In the case of *amyloidogenic proteins*, the product of protein aggregation has been widely demonstrated to be aggregated protein fibrils. However, the pathway by which normal monomeric forms of the protein become fibrils and the intermediate species that are formed along the way, either on- or off-pathway to fibril formation, are still uncertain. Future studies are needed since as a consensus on the structure and toxicity of intermediate species remains elusive.
- Many approaches exist for trying to determine the mechanism(s) and rate constant(s) of protein aggregation. These approaches can be broken broadly into three categories: (i) kinetic and thermodynamic, (ii) other, and (iii) empirical approaches as summarized back in Scheme 2.
- We have focused on reporting, in historical order, the kinetic, thermodynamic, and other approaches that have been used in trying to determine the kinetics and mechanism(s) of protein aggregation. We find that there are five main classes of mechanisms or approaches in the protein aggregation literature: i) subsequent monomer addition, ii) reversible association, iii) prion aggregation mechanisms, iv) the "Ockham's razor"/minimalistic 2-step (F–W) model, and v) quantitative structure–activity relationship models.
- Each of the five classes of kinetic and thermodynamic mechanisms was reviewed in detail, and where possible the fits obtained from the proposed mechanisms and corresponding equations were given to demonstrate how well those mechanisms/models were able to fit protein aggregation kinetic data.
- We applied the concept of "polymerized monomer" originally introduced by Oosawa [78], to the subsequent monomer addition mechanism along with Griffith's and Lansbury's prion mechanisms. This approximation method helps simplify the systems of associated rate equations so that they should become easier to solve.
- In what may prove to be an important part of this review, we expressed where possible the (four) mechanisms of protein aggregation shown in Schemes 21, 22a, 22b, and 23 in terms of common monomer (M) and polymerized monomer (P) terms so that they can be compared, contrasted, and serve as a stepping-stone for future work.
- We also briefly discussed empirical approaches that have been used in the literature. The empirical approaches and resultant equations provide good fits to the kinetic data, but the resultant fitting parameters lack physical meaning, greatly limiting their usefulness.

Acknowledgements

We thank Mr. Steve Hays for his graphic design of the schematic fibril pictured in Scheme 1. We also thank Professors Eric D. Ross and Jeffrey N. Agar for providing their insightful comments on the manuscript. Finally, we gratefully acknowledge NSF grant #0611588 for partial support of this project.

Appendix A. Supplementary data

Supplementary data associated with this article can be found, in the online version, at doi:10.1016/j.bbapap.2008.10.016.

References

[1] K. Blennow, M.J. de Leon, H. Zetterberg, Alzheimer's disease, Lancet 368 (2006) 387–403 and references therein.
[2] G.P. Bates, C. Benn, The polyglutamine diseases, in: G.P. Bates, P.S. Harper, L. Jones (Eds.), Huntington's Disease, Oxford University Press, Oxford, 2002, pp. 429–472.
[3] W. Dauer, S. Przedborski, Parkinson's disease: mechanisms and models, Neuron 39 (2003) 889–909 and references therein.
[4] S.B. Prusiner, Molecular biology of prion diseases, Science 252 (1991) 1515–1522.
[5] L. Morozova-Roche, M. Malisauskas, A false paradise — mixed blessings in the protein universe: the amyloid as a new challenge in drug development, Curr. Med. Chem. 14 (2007) 1221–1230.
[6] J.M. Berg, J.L. Tymoczko, L. Stryer, Actin is a polar, self-assembling, dynamic polymer, Biochemistry, 5th edition, W. H. Freeman, New York, 2002, pp. 958–960.
[7] H. Eisenberg, Glutamate dehydrogenase: anatomy of a regulatory enzyme, Acc. Chem. Res. 4 (1971) 379–385.
[8] D. Thusius, Mechanism of bovine liver glutamate dehydrogenase self-assembly: II. Simulation of relaxation spectra for an open linear polymerization proceeding via a sequential addition of monomer units, J. Mol. Biol. 94 (1975) 367–383.
[9] D. Thusius, P. Dessen, J.-M. Jallon, Mechanism of bovine liver glutamate dehydrogenase self-association I. Kinetic evidence for a random association of polymer chains, J. Mol. Biol. 92 (1975) 413–432.
[10] M. Jullien, D. Thusius, Mechanism of bovine liver glutamate dehydrogenase self-assembly III. Characterization of the association–dissociation stoichiometry with quasi-elastic light scattering, J. Mol. Biol. 101 (1976) 397–416.
[11] C.J. Roberts, Kinetics of irreversible protein aggregation: analysis of extended Lumry–Eyring models and implications for predicting protein shelf life, J. Phys. Chem. B 107 (2003) 1194–1207.
[12] F. Oosawa, S. Asakura, K. Hotta, I. Nobuhisa, T. Ooi, G–F transformation of actin as a fibrous condensation, J. Polym. Sci. 37 (1959) 323–336.
[13] D.M. Walsh, D.J. Selkoe, Aβ oligomers. A decade of discovery, J. Neurochem. 101 (2007) 1172–1184.
[14] C.J. Roberts, Non-native protein aggregation kinetics, Biotechnol. Bioeng. 98 (2007) 927–938.
[15] R.M. Murphy, B.S. Kendrick, Protein misfolding and aggregation, Biotechnol. Prog. 23 (2007) 548–552.
[16] C. Frieden, Protein aggregation processes: in search of the mechanism, Protein Sci. 16 (2007) 2334–2344.
[17] E. van der Linden, P. Venema, Self-assembly and aggregation of proteins, Curr. Opin. Colloid Interface Sci. 12 (2007) 158–165.
[18] J. Gsponer, M. Vendruscolo, Theoretical approaches to protein aggregation, Protein Pept. Lett. 13 (2006) 287–293.
[19] S. Ohnishi, K. Takano, Amyloid fibrils from the viewpoint of protein folding, Cell. Mol. Life Sci. 61 (2004) 511–524.
[20] S.T. Ferreira, M.N.N. Vieira, F.G. De Felice, Soluble protein oligomers as emerging toxins in Alzheimer's and other amyloid diseases, Life 59 (2007) 332–345.
[21] E. Monsellier, F. Chiti, Prevention of amyloid-like aggregation as a driving force of protein evolution, EMBO Rep. 8 (2007) 737–742.
[22] K. Trzesniewska, M. Brzyska, D. Elbaum, Neurodegenerative aspects of protein aggregation, Acta Neurobiol. Exp. 64 (2004) 41–52.
[23] R. Tycko, Insights into the amyloid folding problem from solid-state NMR, Biochemistry 42 (2003) 3151–3159.
[24] D. Foguel, J.L. Silva, New insights into the mechanisms of protein misfolding and aggregation in amyloidogenic diseases derived from pressure studies, Biochemistry 43 (2004) 11361–11370.
[25] R.M. Murphy, Kinetics of amyloid formation and membrane interaction with amyloidogenic proteins, Biochim. Biophys. Acta 1768 (2007) 1923–1934.
[26] M.A. Lauffer, Entropy-driven polymerization of proteins: tobacco mosaic virus protein and other proteins of biological importance, Dev. Biochem. 30 (1978) 115–170.
[27] S.E. Bondos, Methods for measuring protein aggregation, Curr. Anal. Chem. 2 (2006) 157–170.
[28] T.R. Serio, A.G. Cashikar, A.S. Kowal, G.J. Sawicki, J.J. Moslehi, L. Serpell, M.F. Arnsdorf, S.L. Lindquist, Nucleated conformational conversion and the replication of conformational information by a prion determinant, Science 289 (2000) 1317–1321.
[29] M.A. Watzky, A.M. Morris, E.D. Ross, R.G. Finke, Fitting yeast and mammalian prion aggregation kinetic data with the Finke–Watzky 2-step model of nucleation and autocatalytic growth, Biochemistry 47 (2008) 10790–10800.
[30] R. Wetzel, For protein misassembly, it's the "I" decade, Cell 86 (1996) 699–702.
[31] M. Sandal, F. Valle, I. Tessari, S. Mammi, E. Bergantino, F. Musiani, M. Brucale, L. Bubacco, B. Samori, Conformational equilibria in monomeric alpha-synuclein at the single-molecule level, PLoS Biol. 6 (2008) 99–108.
[32] H. Ischiropoulos, Oxidative modifications of alpha-synuclein, Ann. N.Y. Acad. Sci. 991 (2003) 93–100.
[33] B.I. Giasson, J.E. Duda, I.V.J. Murray, Q. Chen, J.M. Souza, H.I. Hurtig, H. Ischiropoulos, J.Q. Trojanowski, V.M.-Y. Lee, Oxidative damage linked to neurodegeneration by selective alpha-synuclein nitration in synucleinopathy lesions, Science 290 (2000) 985–989.
[34] V.N. Uversky, J. Li, A.L. Fink, Evidence for a partially folded intermediate in α-synuclein fibril formation, J. Biol. Chem. 276 (2001) 10737–10744.
[35] V.N. Uversky, A.L. Fink, Conformational constraints for amyloid fibrillation: the importance of being unfolded, Biochim. Biophys. Acta 1698 (2004) 131–153.
[36] A. Dusa, J. Kaylor, S. Edridge, N. Bodner, D.-P. Hong, A.L. Fink, Characterization of oligomers during α-synuclein aggregation using intrinsic tryptophan fluorescence, Biochemistry 45 (2006) 2752–2760.
[37] A.L. Fink, The aggregation and fibrillation of α-synuclein, Acc. Chem. Res. 39 (2006) 628–634.
[38] M. Sunde, L.C. Serpell, M. Bartlam, P.E. Fraser, M.B. Pepys, C.C.F. Blake, Common core structure of amyloid fibrils by synchrotron X-ray diffraction, J. Mol. Biol. 273 (1997) 729–739.
[39] M.F. Perutz, J.T. Finch, J. Berriman, A. Lesk, Amyloid fibers are water-filled nanotubes, Proc. Natl. Acad. Sci. U. S. A. 99 (2002) 5591–5595.
[40] S.B. Malinchik, H. Inouye, K.E. Szumowski, D.A. Kirschner, Biophys. J. 74 (1998) 537–545.
[41] L. Serpell, C.C.F. Blake, P.E. Fraser, Structural analysis of Alzheimer's beta(1–40) amyloid: protofilament assembly of tubular fibrils, Biochemistry 39 (2000) 13269–13275.
[42] W.A. Eaton, J. Hofrichter, Sickle cell hemoglobin polymerization, in: C.B. Anfinsen, J.T. Edsall, F.M. Richards, D.S. Eisenberg (Eds.), Advances in Protein Chemistry, Academic Press, San Diego, 1990.
[43] G. Dykes, R.H. Crepeau, S.J. Edelstein, Three-dimensional reconstruction of the fibres of sickle cell haemoglobin, Nature 272 (1978) 506–510.
[44] G.W. Dykes, R.H. Crepeau, S.J. Edelstein, Three-dimensional reconstruction of the 14-filament fibers of hemoglobin S, J. Mol. Biol. 130 (1979) 451–472.
[45] D.L. Harrington, K. Adachi, W.E. Royer Jr., The high resolution crystal structure of deoxyhemoglobin S, J. Mol. Biol. 272 (1997) 398–407.
[46] C.C. Selby, R.S. Bear, The structure of actin-rich filaments of muscles according to X-ray diffraction, J. Biophys. Biochem. Cytol. 2 (1956) 71–85.
[47] J. Hanson, J. Lowy, The structure of F-actin and of actin filaments isolated from muscle, J. Mol. Biol. 6 (1963) 46–60.
[48] J. Woodhead-Galloway, Structure of collagen fibril: some variations on a theme of tetragonally packed dimmers, Proc. R. Soc. London, B 209 (1980) 275–297.
[49] V. Ottani, D. Martini, M. Franchi, A. Ruggeri, M. Raspanti, Hierarchical structures of fibrillar collagens, Micron 33 (2002) 587–596.
[50] H. Wille, M.D. Michelitsch, V. Guénebaut, S. Supattapone, A. Serban, F.E. Cohen, D. A. Agard, S.B. Prusiner, Structural studies of the scrapie prion protein by electron crystallography, Proc. Natl. Acad. Sci. U. S. A. 99 (2002) 3563–3568.
[51] R. Nelson, M.R. Sawaya, M. Balbirnie, A.O. Madsen, C. Riekel, R. Grothe, D. Eisenberg, Structure of the cross-β spine of amyloid-like fibrils, Nature 435 (2005) 773–778.
[52] O.S. Makin, E. Atkins, P. Sikorski, J. Johansson, L.C. Serpell, Molecular basis for amyloid fibril formation and stability, Proc. Natl. Acad. Sci. U. S. A. 102 (2005) 315–320.
[53] O.S. Makin, L.C. Serpell, Structures for amyloid fibrils, FEBS J. 272 (2005) 5950–5961.
[54] X. Fernandez-Busquets, N.S. de Groot, D. Fernandez, S. Ventura, Recent structural and computational insights into conformational diseases, Curr. Med. Chem. 15 (2008) 1336–1349.
[55] W.S. Gosal, I.J. Morten, E.W. Hewitt, D.A. Smith, N.H. Thomson, S.E. Radford, Competing pathways determine fibril morphology in the self-assembly of beta (2)-microglobulin into amyloid, J. Mol. Biol. 351 (2005) 850–864.
[56] E.T. Powers, D.L. Powers, Mechanism of protein fibril formation: nucleated polymerization with competing off-pathway aggregation, Biophys. J. 94 (2008) 379–391.
[57] H.A. Lashuel, B.M. Petre, J. Wall, M. Simon, R.J. Nowak, T. Walz, P.T. Lansbury Jr., α-Synuclein, especially the Parkinson's disease-associated mutants, forms pore-like annular and tubular protofibrils, J. Mol. Biol. 322 (2002) 1089–1102.
[58] H.A. Lashuel, D. Harley, B.M. Petre, T. Walz, P.T. Lansbury Jr., Amyloid pores from pathogenic mutations, Nature 418 (2002) 291.
[59] T.T. Ding, S.J. Lee, J.-C. Rochet, P.T. Lansbury Jr., Annular α-synuclein protofibrils are produced when spherical protofibrils are incubated in solution or bound to brain-derived membranes, Biochemistry 41 (2002) 10209–10217.
[60] B. Caughey, P.T. Lansbury Jr., Protofibrils, pores, fibrils, and neurodegeneration: separating the responsible protein aggregates from the innocent bystanders, Annu. Rev. Neurosci. 26 (2003) 267–298.
[61] J. Kaylor, N. Bodner, S. Edridge, G. Yamin, D.P. Hong, A.L. Fink, Characterization of oligomeric intermediates in α-synuclein fibrillation: FRET studies of Y125W/Y133F/Y136F α-synuclein, J. Mol. Biol. 353 (2005) 357–372.
[62] M. Zhu, S. Han, F. Zhou, S.A. Carter, A.L. Fink, Annular oligomeric amyloid intermediates observed by in situ atomic force microscopy, J. Biol. Chem. 279 (2004) 24452–24459.
[63] R. Khurana, C. Ionescu-Zanetti, M. Pope, J. Li, L. Nielson, M. Ramirez-Alvarado, L. Regan, A.L. Fink, S.A. Carter, A general model for amyloid fibril assembly based on morphological studies using atomic force microscopy, Biophys. J. 85 (2003) 1135–1144.
[64] G.M. Shankar, S. Li, T.H. Mehta, A. Garcia-Munoz, N.E. Shepardson, I. Smith, F.M. Brett, M.A. Farrell, M.J. Rowan, C.A. Lemere, C.M. Regan, D.M. Walsh, B.L. Sabatini, D.J. Selkoe, Amyloid-β protein dimmers isolated directly from Alzheimer's brains impair synaptic plasticity and memory, Nat. Med. 14 (2008) 837–842.
[65] M.J. Volles, P.T. Lansbury Jr., Zeroing in on the pathogenic form of alpha-synuclein and its mechanism of neurotoxicity in Parkinson's disease, Biochemistry 42 (2003) 7871–7878.

[66] D.A. Butterfield, A. Castegna, C.M. Lauderback, J. Drake, Evidence that amyloid beta-peptide-induced lipid peroxidation and its sequelae in Alzheimer's disease brain contribute to neuronal death, Neurobiol. Aging 23 (2002) 655–664.
[67] B.J. Tabner, S. Turnbull, N.J. Fullwood, M. German, D. Allsop, The production of hydrogen peroxide during early-stage protein aggregation: a common pathological mechanism in different neurodegenerative diseases? Biochem. Soc. Trans. 33 (2005) 548–550.
[68] M.T. Maloney, J.R. Bamburg, Cofilin-mediated neurodegeneration in Alzheimer's disease and other amyloidopathies, Mol. Neurobiol. 35 (2007) 21–44.
[69] C.M. Dobson, Protein aggregation and its consequences for human disease, Protein Pept. Lett. 13 (2006) 219–227.
[70] K.M. Lundberg, C.J. Stenland, F.E. Cohen, S.B. Prusiner, G.L. Millhauser, Kinetics and mechanism of amyloid formation by the prion protein H1 peptide as determined by time-dependent ESR, Chem. Biol. 4 (1997) 345–355.
[71] F. Sokolowski, A.J. Modler, R. Masuch, D. Zirwer, M. Baier, G. Lutsch, D.A. Moss, K. Gast, D. Naumann, Formation of critical oligomers is a key event during conformational transition of recombinant Syrian hamster prion protein, J. Biol. Chem. 278 (2003) 40481–40492.
[72] J. Ollesch, E. Künnemann, R. Glockshuber, K. Gerwert, Prion protein α-to-β transition monitored by time-resolved Fourier transform infrared spectroscopy, Appl. Spectrosc. 61 (2007) 1025–1031.
[73] A. Perálvarez-Marín, A. Barth, A. Gräslund, Time-resolved infrared spectroscopy of pH-induced aggregation of the Alzheimer $A\beta_{1-28}$ peptide, J. Mol. Biol. 379 (2008) 589–596.
[74] M.A. Lauffer, in: A. Kleinzeller, G.F. Springer, H.G. Wittmann (Eds.), Entropy-Driven Processes in Biology: Polymerization of Tobacco Mosaic Virus Protein And Similar Reactions, Springer-Verlag, Berlin, 1975.
[75] S.S. Licht, C.C. Lawrence, J. Stubbe, Thermodynamic and kinetic studies on carbon–cobalt bond homolysisby ribonucleoside triphosphate reductase: the importance of entropy in catalysis, Biochemistry 38 (1999) 1234–1242.
[76] A.M. Morris, M.A. Watzky, J.N. Agar, R.G. Finke, Fitting neurological protein aggregation kinetic data via a 2-step minimal/"Ockham's razor" model: the Finke–Watzky mechanism of nucleation followed by autocatalytic surface growth, Biochemistry 47 (2008) 2413–2427.
[77] M. Kasai, S. Asakura, F. Oosawa, The cooperative nature of G–F transformation of actin, Biochim. Biophys. Acta 57 (1962) 22–31.
[78] F. Oosawa, M. Kasai, A theory of linear and helical aggregations of macromolecules, J. Mol. Biol. 4 (1962) 10–21.
[79] F. Oosawa, Size distribution of protein polymers, J. Theor. Biol. 27 (1970) 69–86.
[80] J. Hofrichter, P.D. Ross, W.A. Eaton, Kinetics and mechanism of deoxyhemoglobin S gelation: a new approach to understanding sickle cell disease, Proc. Natl. Acad. Sci. U. S. A. 71 (1974) 4864–4868.
[81] M. Saunders, P.D. Ross, A simple model of the reaction between polyadenylic acid and polyuridylic acid, Biochem. Biophys. Res. Commun. 3 (1960) 314–318.
[82] V.K. La Mer, Nucleation in phase transitions, Ind. Eng. Chem. 44 (1952) 1270–1277.
[83] F.A. Ferrone, J. Hofrichter, H.R. Sunshine, W.A. Eaton, Kinetic studies on photolysis-induced gelation of sickle cell hemoglobin suggest a new mechanism, Biophys. J. 32 (1980) 361–377.
[84] A. Wegner, J. Engel, Kinetics of the cooperative association of actin to actin filaments, Biophys. Chem. 3 (1975) 215–225.
[85] L.S. Tobacman, E.D. Korn, The kinetics of actin nucleation and polymerization, J. Biol. Chem. 258 (1983) 3207–3214.
[86] C. Frieden, D.W. Goddette, Polymerization of actin and actin-like systems: evaluation of the time course of polymerization in relation to the mechanism, Biochemistry 22 (1983) 5836–5843.
[87] M.P. Firestone, R. De Levie, S.K. Rangarajan, On one-dimensional nucleation and growth of "living" polymers I. Homogeneous nucleation, J. Theor. Biol. 104 (1983) 553–570.
[88] S.K. Rangarajan, R. De Levie, On one-dimensional nucleation and growth of "living" polymers II. Growth at constant monomer concentration, J. Theor. Biol. 104 (1983) 553–570.
[89] M.A. Watzky, R.G. Finke, Transition metal nanocluster formation kinetic and mechanistic studies. A new mechanism when hydrogen is the reductant: slow, continuous nucleation and fast autocatalytic surface growth, J. Am. Chem. Soc. 119 (1997) 10382–10400.
[90] R.F. Goldstein, L. Stryer, Cooperative polymerization reactions: analytical approximations, numerical examples, and experimental strategy, Biophys. J. 50 (1986) 583–599.
[91] F. Oosawa, S. Asakura, Kinetics of polymerization 4. Fragmentation and association of polymers, in: B. Horecker, N.O. Kaplan, J. Marmur, H.A. Scheraga (Eds.), Thermodynamics of the Polymerization of Protein, 55, Academic Press, New York, 1975.
[92] A. Wegner, P. Savko, Fragmentation of actin filaments, Biochemistry 21 (1982) 1909–1913.
[93] P.O.P. Ts'o, I.S. Melvin, A.C. Olson, Interaction and association of bases and nucleosides in aqueous solutions, J. Am. Chem. Soc. 85 (1963) 1289–1296.
[94] K.E. Van Holde, G.P. Rossetti, A sedimentation equilibrium study of the association of purine in aqueous solutions, Biochemistry 6 (1967) 2189–2194.
[95] E.T. Adams Jr., M.S. Lewis, Sedimentation equilibrium in reacting systems. VI. Some applications to indefinite self-association. Studies with β-lactoglobulin A, Biochemistry 7 (1968) 1044–1053.
[96] E. Reisler, J. Pouyet, H. Eisenberg, Molecular weights, association, and frictional resistance of bovine liver glutamate dehydrogenase at low concentrations. Equilibrium and velocity sedimentation, light-scattering studies, and settling experiments with macroscopic models of the enzyme oligomer, Biochemistry 9 (1970) 3095–3102.
[97] M. Eigen, Prionics or the kinetic basis of prion diseases, Biophys. Chem. 63 (1996) A1–A18.
[98] J.S. Griffith, Self-replication and scrapie, Nature 215 (1967) 1043–1044.
[99] S.B. Prusiner, Novel proteinaceous infectious particles cause scrapie, Science 216 (1982) 136–144.
[100] F.E. Cohen, K.-M. Pan, Z. Huang, M. Baldwin, R.J. Fletterick, S.B. Prusiner, Structural clues to prion replication, Science 264 (1994) 530–531.
[101] I.V. Baskakov, G. Legname, M.A. Baldwin, S.B. Prusiner, F.E. Cohen, Pathway complexity of prion protein assembly into amyloid, J. Biol. Chem. 277 (2002) 21140–21148.
[102] M. Laurent, Autocatalytic processes in cooperative mechanisms of prion diseases, FEBS Lett. 407 (1997) 1–6.
[103] J.T. Jarrett, P.T. Lansbury Jr., Seeding "one-dimensional crystallization" of amyloid: a pathogenic mechanism in Alzheimer's disease and scrapie? Cell 73 (1993) 1055–1058.
[104] J.H. Come, P.E. Fraser, P.T. Lansbury Jr., A kinetic model for amyloid formation in prion diseases: importance of seeding, Proc. Natl. Acad. Sci. U. S. A. 90 (1993) 5959–5963.
[105] P.T. Lansbury Jr., B. Caughey, The chemistry of scrapie infection: implications of the 'ice 9' metaphor, Chem. Biol. 2 (1995) 1–5.
[106] B. Caughey, D.A. Kocisko, G.J. Raymond, P.T. Lansbury Jr., Aggregates of scrapie-associated prion protein induce the cell-free conversion of protease-sensitive prion protein to the protease-resistant state, Chem. Biol. 2 (1995) 807–817.
[107] T. Scheibel, J. Bloom, S.L. Lindquist, The elongation of yeast prion fibers involves separable steps of association and conversion, Proc. Natl. Acad. Sci. U. S. A. 101 (2004) 2287–2292.
[108] H. Flyvbjerg, E. Jobs, S. Leibler, Kinetics of self-assembling microtubules: an "inverse problem" in biochemistry, Proc. Natl. Acad. Sci. U. S. A. 93 (1996) 5975–5979.
[109] A. Lomakin, D.S. Chung, G.B. Benedek, D.A. Kirschner, D.B. Teplow, On the nucleation and growth of amyloid β-protein fibrils: detection of nuclei and quantitation of rate constants, Proc. Natl. Acad. Sci. U. S. A. 93 (1996) 1125–1129.
[110] R. Kayed, E. Head, J.L. Thompson, T.M. McIntire, S.C. Milton, C.W. Cotman, C.G. Glabe, Common structure of soluble amyloid oligomers implies common mechanism of pathogenesis, Science 300 (2003) 486–489.
[111] A. Lomakin, D.B. Teplow, D.A. Kirschner, G.B. Benedek, Kinetic theory of fibrillogenesis of amyloid β-protein, Proc. Natl. Acad. Sci. U. S. A. 94 (1997) 7942–7947.
[112] M.M. Pallitto, R.M. Murphy, A mathematical model of the kinetics of beta-amyloid fibril growth from the denatured state, Biophys. J. 81 (2001) 1805–1822.
[113] F.A. Ferrone, Analysis of protein aggregation kinetics, Methods Enzymol. 309 (1999) 256–274.
[114] M.F. Bishop, F.A. Ferrone, Kinetics of nucleation-controlled polymerization, Biophys. J. 46 (1984) 631–644.
[115] S. Chen, F.A. Ferrone, R. Wetzel, Huntington's disease age-of-onset linked to polyglutamine aggregation nucleation, Proc. Natl. Acad. Sci. 99 (2002) 11884–11889.
[116] R. Wetzel, Kinetics and thermodynamics of amyloid fibril assembly, Acc. Chem. Res. 39 (2006) 671–679.
[117] T. Cellmer, R. Douma, A. Huebner, J. Prausnitz, H. Blanch, Kinetic studies of protein L aggregation and disaggregation, Biophys. Biochem. 125 (2007) 350–359.
[118] C.C. Lee, R.H. Walters, R.M. Murphy, Reconsidering the mechanism of polyglutamine peptide aggregation, Biochemistry 46 (2007) 12810–12820.
[119] R. Lumry, H. Eyring, Conformation changes of proteins, J. Phys. Chem. 58 (1954) 110–120.
[120] J.M. Andrews, C.J. Roberts, A Lumry–Eyring nucleated polymerization model of protein aggregation kinetics: 1. Aggregation with pre-equilibrated unfolding, J. Phys. Chem. B 111 (2007) 7897–7913.
[121] C.J. Roberts, The kinetics of nucleated polymerizations at high concentrations: amyloid fibril formation near and above the "supercritical concentration, in: R.M. Murphy, A.M. Tsai (Eds.), Misbehaving Proteins: Protein (Mis)Folding, Aggregation and Stability, Springer, New York, 2006, pp. 17–46.
[122] J.M. Andrews, C.J. Roberts, Non-native aggregation of alpha-chymotrypsinogen occurs through nucleation and growth with competing nucleus sizes and negative activation energies, Biochemistry 46 (2007) 7558–7571.
[123] W.F. Weiss IV, T.K. Hogdon, E.W. Kaler, A.M. Lenhoff, C.J. Roberts, Nonnative protein polymers: structure, morphology, and relation to nucleation and growth, Biophys. J. 93 (2007) 4392–4403.
[124] J.M. Andrews, W.F. Weiss IV, C.J. Roberts, Nucleation, growth, and activation energies for seeded and unseeded aggregation of alpha-chymotrypsinogen A, Biochemistry 47 (2008) 2397–2403.
[125] E.T. Powers, D.L. Powers, The kinetics of nucleated polymerizations at high concentrations: amyloid fibril formation near and above the "supercritical concentration", Biophys. J. 91 (2006) 122–132.
[126] William of Ockham, 1285–1349, as cited by E.A. Moody in, The Encyclopedia of Philosophy, vol 7, McMillan, 1967.
[127] M. Kamihira, A. Naito, S. Tuzi, A. Nosaka, H. Saitô, Conformational transitions and fibrillation mechanism of human calcitonin as studied by high-resolution solid-state ^{13}C NMR, Protein Sci. 9 (2000) 867–877.
[128] S.S.-S. Wang, Y.-T. Chen, P.-H. Chen, K.-N. Liu, A kinetic study on the aggregation behavior of beta-amyloid peptides in different initial solvent environments, Biochem. Eng. J. 29 (2006) 129–138.

[129] M.-S. Lin, L.-Y. Chen, H.-T. Tsai, S.S.-S. Wang, Y. Chang, A. Higuchi, W.-Y. Chen, Investigation of the mechanism of β-amyloid fibril formation by kinetic and thermodynamic analyses, Langmuir 24 (2008) 5802–5808.
[130] R. Sabaté, M. Gallardo, J. Estelrich, An autocatalytic reaction as a model for the kinetics of the aggregation of β-amyloid, Biopolymers 71 (2003) 190–195.
[131] R. Sabaté, J. Estelrich, Stimulatory and inhibitory effects of alkyl bromide surfactants on beta-amyloid fibrillogenesis, Langmuir 21 (2005) 6944–6949.
[132] R. Sabaté, M. Gallardo, J. Estelrich, Spontaneous incorporation of β-amyloid peptide into neutral liposomes, Colloids Surf., A 270–271 (2005) 13–17.
[133] R. Sabaté, U. Baxa, L. Benkemoun, N. Sánchez de Groot, B. Coulary-Salin, M.-L. Maddelein, L. Malato, S. Ventura, A.C. Steven, S.J. Saupe, Prion and non-prion amyloids of the HET-s prion forming domain, J. Mol. Biol. 370 (2007) 768–783.
[134] T.J. Gibson, R.M. Murphy, Inhibition of insulin fibrillogenesis with targeted peptides, Protein Sci. (2006) 1133–1141.
[135] F. Chiti, M. Stefani, N. Taddei, G. Ramponi, C.M. Dobson, Rationalization of the effects of mutations on peptide and protein aggregation rates, Nature 424 (2003) 805–808.
[136] K.F. DuBay, A.P. Pawar, F. Chiti, J. Zurdo, C.M. Dobson, M. Vendruscolo, Prediction of the absolute aggregation rates of amyloidogenic polypeptide chains, J. Mol. Biol. 341 (2004) 1317–1326.
[137] H. Naiki, K. Nakakuki, First-order kinetic model of Alzheimer's β-amyloid fibril extension in vitro, Lab. Invest. 74 (1996) 374–383.
[138] K. Hasegawa, K. Ono, M. Yamada, H. Naiki, Kinetic modeling and determination of reaction constants of Alzheimer's β-amyloid fibril extension and dissociation using surface plasmon resonance, Biochemistry 41 (2002) 13489–13498.
[139] H. Naiki, F. Gejyo, Kinetic analysis of amyloid fibril formation, Methods Enzymol. 309 (1999) 305–318.
[140] L.C. Cerny, D.M. Stasiw, W. Zuk, The logistic curve for fitting sigmoidal data, Physiol. Chem. Phys. 13 (1981) 221–230.
[141] J.S. Pedersen, D. Dikov, J.L. Flink, H.A. Hjuler, G. Christiansen, D.E. Otzen, The changing face of glucagon fibrillation: structural polymorphism and conformational imprinting, J. Mol. Biol. 355 (2006) 501–523.
[142] L. Nielsen, R. Khurana, A. Coats, S. Frokjaer, J. Brange, S. Vyas, V.N. Uversky, A.L. Fink, Effect of environmental factors on the kinetics of insulin fibril formation: elucidation of the molecular mechanism, Biochemistry 40 (2001) 6036–6046.
[143] F.J. Richards, A flexible growth function for empirical use, J. Exp. Bot. 10 (1959) 290–300.
[144] X.Y. Yin, J. Goudriaan, E.A. Lantinga, J. Vos, H.J. Spiertz, A flexible sigmoid function of determinate growth, Ann. Bot. 91 (2003) 361–371.
[145] C.-C. Lee, A. Nayak, A. Sethuraman, G. Belfort, G.J. McRae, A three-stage kinetic model of amyloid fibrillation, Biophys. J. 92 (2007) 3448–3458.
[146] J.R. Platt, Strong inference: certain systematic methods of scientific thinking may produce much more rapid progress than others, Science 146 (1964) 347–353.
[147] H. Kacser, J.R. Small, How many phenotypes from one genotype? The case of prion diseases, J. Theor. Biol. 182 (1996) 209–218.
[148] F.A. Ferrone, Nucleation: the connections between equilibrium and kinetic behavior, Methods Enzymol. 412 (2006) 285–299.
[149] J.D. Harper, P.T. Lansbury Jr., Models of amyloid seeding in Alzheimer's disease and scrapie: mechanistic truths and physiological consequences of the time-dependent solubility of amyloid proteins, Annu. Rev. Biochem. 66 (1997) 385–407.
[150] C. LeBlond, J. Wang, R.D. Larsen, C.J. Orella, A.L. Forman, R.N. Landau, J. Laquidara, J.R. Sowa Jr., D.G. Blackmond, Y.-K. Sun, Reaction calorimetry as an in-situ kinetic tool for characterizing complex reactions, Thermochim. Acta 289 (1996) 189–207.
[151] R.W. Woody, Theory of circular dichroism of proteins, in: G.D. Fasman (Ed.), Theory of Circular Dichroism of Proteins in Circular Dichroism and the Conformational Analysis of Biomolecules, Plenum Press, New York, 1996, pp. 25–68.
[152] L.A. Munishkina, A.L. Fink, Fluorescence as a method to reveal structures and membrane-interactions of amyloidogenic proteins, Biochim. Biophys. Acta 1768 (2007) 1862–1885.
[153] F. Oosawa, S. Asakura, K. Hotta, I. Nobuhisa, T. Ooi, G–F transformation of actin as a fibrous condensation, J. Polym. Sci. 37 (1959) 323–336.
[154] M. Kasai, F. Oosawa, Flow birefringence, Methods Enzymol. 26 (1972) 289–323.
[155] S.P.F.M. Roefs, K.G. De Kruif, A model for the denaturation and aggregation of beta-lactoglobulin, Eur. J. Biochem. 226 (1994) 883–889.
[156] S.F. Sun, Diffusion, light scattering, Physical Chemistry of Macromolecules: Basic Principles and Issues, 2nd Ed., Wiley and Sons, New York, 2004, pp. 223–242.
[157] M. Moniatte, F.G. van der Goot, J.T. Buckley, F. Pattus, A. van Dorsselaer, Characterisation of the heptameric pore-forming complex of the Aeromonas toxin aerolysin using MALDI-TOF mass spectrometry, FEBS Lett. 384 (1996) 269–272.
[158] W.J. Henzel, J.T. Stults, Matrix-assisted laser desorption/ionization time-of-flight mass analysis of peptides, in: J.E. Coligan, B.M. Dunn, H.L. Ploegh, D.W. Speicher, P.T. Wingfield (Eds.), Current Protocols in Protein Science, Wiley and Sons, New York, 2004, Unit 16.2.
[159] C.O. Fernandéz, W. Hoyer, M. Zweckstetter, E.A. Jares-Erijman, V. Subramaniam, C. Griesinger, T.M. Jovin, NMR of alpha-synuclein–polyamine complexes elucidates the mechanism and kinetics of induced aggregation, EMBO J. 23 (2004) 2039–2046.
[160] T.P.J. Knowles, W. Shu, G.L. Devlin, S. Meehan, S. Auer, C.M. Dobson, M.E. Welland, Kinetics and thermodynamics of amyloid formation from direct measurements of fluctuations in fibril mass, Proc. Natl. Acad. Sci. U. S. A. 104 (2007) 10016–10021.
[161] B.J. Berne, Interpretation of the light scattering from long rods, J. Mol. Biol. 89 (1974) 755–758.
[162] S.E. Harding, The intrinsic viscosity of biological macromolecules. Progress in measurement, interpretation and application to structure in dilute solution, Prog. Biophys. Mol. Biol. 68 (1997) 207–262.
[163] A.M. Morris, R.G. Finke, alpha-synuclein aggregation variable temperature and variable pH kinetic data: A reanalysis using the Finke-Watzky 2-step model of nucleation and autocatalytic growth, Biophys. Chem. (in press).